



Box integrals with fermion bubbles for low-energy measurements of the weak mixing angle

Nico Böttcher, Niklas Schwanemann, Stefan Weinzierl^a

PRISMA Cluster of Excellence, Institut für Physik Johannes Gutenberg-Universität Mainz, 55099 Mainz, Germany

Received: 13 December 2023 / Accepted: 22 April 2024
© The Author(s) 2024

Abstract The Moller experiment and the P2 experiment aim at measuring the weak mixing angle at low scales. The Moller experiment uses $e^-e^- \rightarrow e^-e^-$ -scattering, the P2 experiment uses $e^-N \rightarrow e^-N$ -scattering. In both cases, two-loop electroweak corrections have to be taken into account, and here in particular diagrams which give rise to large logarithms. In this paper we compute a set of two-loop electroweak Feynman integrals for point-like particles, which are obtained from a box integral by the insertion of a light fermion loop. By rationalising all occurring square roots we show that these Feynman integrals can be expressed in terms of multiple polylogarithms. We present the results in a form, which makes the large logarithms manifest. We provide highly efficient numerical evaluation routines for these integrals.

1 Introduction

The Moller experiment [1] at Jefferson Lab and the P2 experiment [2] at the MESA accelerator at Mainz University will measure the weak mixing angle at low scales. The process studied at the Moller experiment is electron–electron scattering, the process studied at the P2 experiment is electron–nucleon scattering. In both cases, the experimental programs require theory input in the form of precision calculations.

Of particular importance are diagrams, which give rise to large logarithms. Neglecting the electron mass, we have for both experiments the hierarchy of scales

$$-t \ll s \sim m_N^2 \ll m_W^2 \sim m_Z^2, \quad (1)$$

where s and t are the Mandelstam variables, m_N the nucleon mass (only relevant for the P2 experiment) and m_W and m_Z the mass of the W -boson and Z -boson, respectively. Large

logarithms arise due to the smallness of $(-t)$ and/or due to the large mass of the heavy gauge bosons. In this paper we consider a box diagram for point-like particles with the insertion of a light fermion loop both for the Moller experiment and the P2 experiment. This diagram is shown in Fig. 1. The wavy lines in this diagram may either be photons (massless) or heavy gauge bosons. In the case of Møller scattering the green line in Fig. 1 is massless, for $e^-N \rightarrow e^-N$ -scattering the green line in Fig. 1 is massive with mass m_N . Depending on the mass configuration we have to calculate in total eight different cases, which we label topology A to topology H . The case where all lines are massless is rather easy. This case will be labelled as topology H . The opposite case, where all wavy lines have the mass of a heavy gauge boson (say m_Z) and the green line has the mass m_N is rather involved and state-of-the-art in Feynman integral calculations. The complication arises from four square roots, which are associated with this topology. This latter case will be labelled as topology A . We compute the master integrals for all topologies A – H .

As a side remark we note that crossing the diagrams with a massive green line gives diagrams relevant to two-loop electroweak corrections and mixed two-loop QCD/electroweak corrections to the production of a pair of heavy particles at the LHC.

In this paper we perform an analytic calculation of these Feynman integrals. We note that a subset of these integrals together with other related integrals have been computed previously with numerical methods [3–7] or asymptotic approximations [8,9].

We compute the Feynman integrals with the help of the method of differential equations [10–12]: Using integration-by-parts identities [13] we first derive a differential equation for a pre-canonical basis of master integrals. This differential equation is in general not in an ε -factorised form. We then construct a new basis, such that the differential equa-

^ae-mail: weinzierl@uni-mainz.de (corresponding author)

tion is transformed to an ε -factorised form [14]. In doing so, we unavoidably need to introduce square roots. In total we encounter five different square roots. It is advisable to treat each topology separately, as not all five square roots occur simultaneously in a given topology. The most complicated case is topology *A* with four occurring square roots. For every topology we may simultaneously rationalise all occurring square roots. This shows that the Feynman integrals can be expressed in terms of multiple polylogarithms. Furthermore, by choosing an appropriate boundary point and by isolating trailing zeros in powers of single logarithms we may make all large logarithms manifest. For all topologies we provide a highly efficient numerical C++-program, which evaluates the master integrals in the kinematic region of interest with arbitrary precision.

For phenomenological applications our results can be used as follows: Let us first consider the case of Møller scattering. It is well-known that all occurring Feynman integrals in a scattering amplitude can be reduced to master integrals. Standard integration-by-parts reduction programs like FIRE/Litered [15–18], Reduze [19,20], Kira [21,22] or FiniteFlow [23,24] facilitate this task. In general, these programs reduce Feynman integrals to a pre-canonical basis of master integrals. Our starting point is the default choice of Kira for a pre-canonical basis of master integrals. The integration-by-parts reduction programs can be used to convert this basis to any other pre-canonical basis. The pre-canonical basis is related by a rotation matrix to the basis of uniform transcendent weight constructed in this paper. The rotation matrix and its inverse are given in the supplementary electronic file attached to the arxiv version of this article. The master integrals of uniform transcendent weight are computed with the provided C++-programs, again given in the supplementary electronic file attached to the arxiv version of this article.

The case of electron-nucleon scattering has additional complications due to the hadronic nature of the nucleon. For the details how calculations are done in this situation we refer to Refs. [25–33]. The main interest is the coefficient of the large logarithm related to the heavy boson mass and we provide the master integrals to extract this coefficient. Let us emphasise that although our calculation is with point-like particles, the inclusion of form factors for the coupling of a nucleon to a gauge boson is straightforward, as long as the form factors are modelled by rational functions in the momenta, which do not introduce new singularities. On the other hand, the inclusion of a nucleon resonance introduces another kinematic variable and leads to loop integrals beyond the ones considered in this paper.

This paper is organised as follows: In Sect. 2 we show that due to partial fractioning we only need to compute a reduced graph. In Sect. 3 we introduce the notation for the Feynman integrals. In Sect. 4 we present for all topologies a basis of

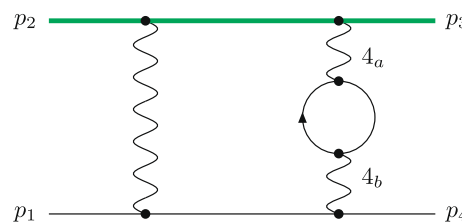


Fig. 1 The two-loop Feynman graph. Wavy lines are either photons (massless) or heavy gauge bosons (massive). The mass of the green line is either zero (this case corresponds to the Møller experiment) or massive with mass m_N (this case corresponds to the P2 experiment). All other particles are assumed to be massless

master integrals of uniform transcendent weight. In Sect. 5 we give the differential equation for each topology and list all differential one-forms appearing in the differential equations. The differential one-forms are dlog-forms with algebraic functions as argument. The algebraic part is given by five square roots. In total we encounter five different square roots. In Sect. 6 we show that for each topology all occurring square roots can be rationalised. As a consequence, all Feynman integrals can be expressed in terms of multiple polylogarithms. In order to solve the differential equations, we need boundary values. These are given in Sect. 7. In Sect. 8 we present numerical results and the leading large logarithms. Finally, our conclusions are given in Sect. 9. In Appendix A we show for all master integrals the corresponding diagrams. In Appendix B we describe the content of the supplementary electronic file attached to the arxiv version of this article. In Appendix C we collect for convenience the corresponding one-loop integrals in the same notation as used for the two-loop integrals.

2 Preliminaries

We are interested in the Feynman graph shown in Fig. 1. The green line could either be a massless fermion or a nucleon (with non-zero mass m_N).

The wavy lines are either massless gauge bosons (photons) or massive gauge bosons (Z -bosons or W -bosons). We are in particular interested in the case, where at least one of the wavy lines is a massive gauge boson. The case where all of them are photons is significantly simpler and only included for completeness. The black solid lines correspond to massless fermions. For $e^-e^- \rightarrow e^-e^-$ -scattering we take the green line to be massless, for $e^-N \rightarrow e^-N$ -scattering we take the green line to be massive. It is sufficient to focus on the case, where the heavy gauge boson is the Z -boson. As we neglect the electron mass, electrons and neutrinos both have zero mass. Furthermore we do not distinguish between the proton and the neutron mass. With these approximations the case with heavy W -bosons gives rise to exactly the same

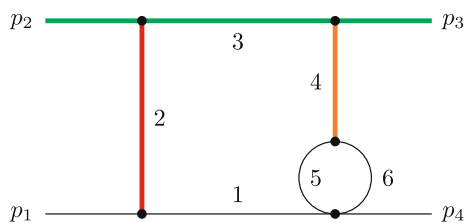


Fig. 2 The reduced Feynman graph

integrals. In the following we will denote the heavy gauge boson mass by m_Z .

We recall that any tensor integral can be reduced to scalar integrals [34,35]. Therefore, although we are interested in integrals with fermions and gauge bosons, what we have to calculate are scalar integrals.

There is one immediate simplification: The momenta flowing through the propagators labelled 4_a and 4_b in Fig. 1 are the same. The two propagators may have equal mass (either $m_{4_a} = m_{4_b} = 0$ or $m_{4_a} = m_{4_b} = m_Z$) or unequal mass (either $m_{4_a} = 0, m_{4_b} = m_Z$ or $m_{4_a} = m_Z, m_{4_b} = 0$). In the latter case we may use partial fraction decomposition

$$\frac{1}{(-q^2 + m_{4_a}^2)(-q^2 + m_{4_b}^2)} = \frac{1}{m_{4_b}^2 - m_{4_a}^2} \left[\frac{1}{(-q^2 + m_{4_a}^2)} - \frac{1}{(-q^2 + m_{4_b}^2)} \right]. \quad (2)$$

We therefore have to consider only the reduced topology shown in Fig. 2 with

$$m_2, m_4 \in \{0, m_Z\}, \quad m_3 \in \{0, m_N\}. \quad (3)$$

The external momenta satisfy

$$p_1^2 = p_4^2 = 0, \quad p_2^2 = p_3^2 = m_3^2. \quad (4)$$

We denote the Mandelstam variables by

$$\begin{aligned} s &= (p_1 + p_2)^2, \\ t &= (p_2 + p_3)^2, \\ u &= (p_1 + p_3)^2. \end{aligned} \quad (5)$$

3 Notation

We need to consider an auxiliary graph associated to the reduced graph of Fig. 2, such that any scalar product involving at least one loop momentum can be expressed as a linear combination of inverse propagators. With three independent external momenta and two independent loop momenta this associated graph must have nine internal propagators. We therefore consider the family of integrals

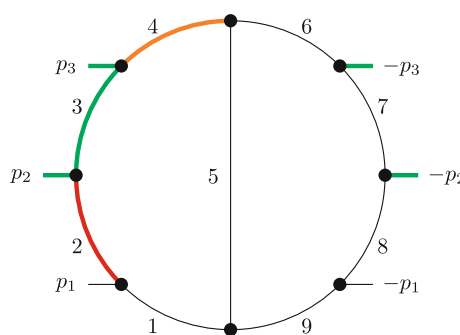


Fig. 3 The auxiliary graph. Green lines correspond to a particle with mass m_3 , orange lines correspond to a particle with mass m_4 and red lines correspond to a particle with mass m_2

$$\begin{aligned} I_{\nu_1 \nu_2 \nu_3 \nu_4 \nu_5 \nu_6 \nu_7 \nu_8 \nu_9} &= e^{2\gamma_E \varepsilon} (\mu^2)^{\nu-D} \int \frac{d^D k_1}{i\pi^{\frac{D}{2}}} \frac{d^D k_2}{i\pi^{\frac{D}{2}}} \prod_{j=1}^9 \frac{1}{P_j^{\nu_j}}, \end{aligned} \quad (6)$$

where γ_E denotes the Euler–Mascheroni constant, $D = 4 - 2\varepsilon$ is the number of space-time dimensions, μ is an arbitrary scale introduced to render the Feynman integral dimensionless and the quantity ν is given by

$$\nu = \sum_{j=1}^9 \nu_j. \quad (7)$$

We will further use the notation $p_{ij} = p_i + p_j$, $p_{ijk} = p_i + p_j + p_k$. The inverse propagators are given by

$$\begin{aligned} P_1 &= -k_1^2, & P_2 &= -(k_1 - p_1)^2 + m_2^2, \\ P_3 &= -(k_1 - p_{12})^2 + m_3^2, \\ P_4 &= -(k_1 - p_{123})^2 + m_4^2, & P_5 &= -k_2^2, \\ P_6 &= -(k_1 + k_2 - p_{123})^2, \\ P_7 &= -(k_1 + k_2 + p_{12})^2, \\ P_8 &= -(k_1 + k_2 - p_1)^2, \\ P_9 &= -(k_1 + k_2)^2. \end{aligned} \quad (8)$$

The graph for this family is shown in Fig. 3.

We are interested in the sectors, for which we have

$$\nu_7, \nu_8, \nu_9 \leq 0. \quad (9)$$

We define a sector id (or topology id) by

$$\text{id} = \sum_{j=1}^9 2^{j-1} \Theta \left(\nu_j - \frac{1}{2} \right). \quad (10)$$

Here, $\Theta(x)$ denotes the Heaviside step function. Since we assume $\nu_j \in \mathbb{Z}$, the shift by $(-1/2)$ avoids any ambiguity in the definition of $\Theta(0)$.

We have to consider eight cases, depending on whether the masses (m_2, m_3, m_4) are non-zero or zero. We define eight topologies

Table 1 The number of master integrals for a given topology

Topology	Master integrals	Topology	Master integrals
A	15	E	10
B	11	F	7
C	8	G	5
D	5	H	3

Table 2 The various roots appearing in a given topology

Topology	Roots	Topology	Roots
A	r_1, r_2, r_3, r_5	E	r_2, r_4
B	r_1, r_3	F	–
C	r_1, r_3	G	–
D	r_1	H	–

$$\begin{aligned}
 A : (m_2, m_3, m_4) &= (m_Z, m_N, m_Z), \\
 E : (m_2, m_3, m_4) &= (m_Z, 0, m_Z), \\
 B : (m_2, m_3, m_4) &= (0, m_N, m_Z), \\
 F : (m_2, m_3, m_4) &= (0, 0, m_Z), \\
 C : (m_2, m_3, m_4) &= (m_Z, m_N, 0), \\
 G : (m_2, m_3, m_4) &= (m_Z, 0, 0), \\
 D : (m_2, m_3, m_4) &= (0, m_N, 0), \\
 H : (m_2, m_3, m_4) &= (0, 0, 0).
 \end{aligned} \tag{11}$$

We write

$$I_{v_1 v_2 v_3 v_4 v_5 v_6 v_7 v_8 v_9}^X, \quad X \in \{A, B, C, D, E, F, G, H\} \tag{12}$$

to denote the corresponding integrals.

The total number of master integrals for the various topologies are shown in Table 1.

In defining master integrals of uniform transcendent weight we will encounter five square roots.

These are given by

$$\begin{aligned}
 r_1 &= \sqrt{-t(4m_N^2 - t)}, \\
 r_2 &= \sqrt{-t(4m_Z^2 - t)}, \\
 r_3 &= \sqrt{-m_Z^2(4m_N^2 - m_Z^2)}, \\
 r_4 &= \sqrt{st[st - 4m_Z^2(m_Z^2 + s)]}, \\
 r_5 &= \sqrt{-t[-t(m_N^2 - s)^2 + 4m_Z^2(m_Z^2 s + (m_N^2 - s)^2)]}.
 \end{aligned} \tag{13}$$

We have chosen the arguments of the five square roots such that in the region of interest ($t < 0, s > 0, m_Z^2 \gg m_N^2, s, (-t)$) the arguments of all five roots are positive. In this region we chose the sign of the square roots such that all

five roots are positive. Table 2 shows for each topology the roots appearing in this topology.

The first graph polynomial [36] for the auxiliary graph shown in Fig. 3 reads

$$\begin{aligned}
 \mathcal{U}(a_1, a_2, a_3, a_4, a_5, a_6, a_7, a_8, a_9) \\
 = (a_1 + a_2 + a_3 + a_4)(a_6 + a_7 + a_8 + a_9) \\
 + a_5(a_1 + a_2 + a_3 + a_4 + a_6 + a_7 + a_8 + a_9).
 \end{aligned} \tag{14}$$

We introduce an operator \mathbf{i}^+ , which raises the power of the propagator i by one and multiplies by v_i , e.g.

$$\mathbf{i}^+ I_{v_1 v_2 v_3 v_4 v_5 v_6 v_7 v_8 v_9} = v_1 \cdot I_{(v_1+1)v_2 v_3 v_4 v_5 v_6 v_7 v_8 v_9}. \tag{15}$$

The notation with an extra prefactor v_j follows Ref. [37]. In addition we define the operator \mathbf{D}^- , which lowers the dimension of space-time by two units through

$$\mathbf{D}^- I_{v_1 v_2 v_3 v_4 v_5 v_6 v_7 v_8 v_9}(D) = I_{v_1 v_2 v_3 v_4 v_5 v_6 v_7 v_8 v_9}(D - 2). \tag{16}$$

The dimensional shift relations read [34,35]

$$\begin{aligned}
 \mathbf{D}^- I_{v_1 v_2 v_3 v_4 v_5 v_6 v_7 v_8 v_9}(D) \\
 = \mathcal{U}(\mathbf{1}^+, \mathbf{2}^+, \mathbf{3}^+, \mathbf{4}^+, \mathbf{5}^+, \mathbf{6}^+, \mathbf{7}^+, \mathbf{8}^+, \mathbf{9}^+) \\
 I_{v_1 v_2 v_3 v_4 v_5 v_6 v_7 v_8 v_9}(D).
 \end{aligned} \tag{17}$$

4 The master integrals

We will treat each topology separately. The main motivation is that this allows us to rationalise for each topology all occurring square roots. This introduces a small redundancy, as the same sub-sectors may occur in more than one topology. This redundancy provides an additional cross-check, as the sub-sectors are computed with different rationalisations and different integration paths.

4.1 Pre-canonical master integrals

Standard integration-by-parts reduction programs like FIRE/Litered [15–18], Reduze [19,20], Kira [21,22] or FiniteFlow [23,24] are capable to express any relevant scalar Feynman integral as a linear combination of master integrals. The chosen master integrals depend on the ordering criteria in the Laporta algorithm [38]. In general, the chosen master integrals are not of uniform weight. Possible pre-canonical bases are:

$$\begin{aligned}
 I^A &= \left(I_{010011000}^A, I_{(-1)10011000}^A, I_{001011000}^A, \right. \\
 &\quad I_{000111000}^A, I_{101011000}^A, I_{011011000}^A, I_{(-1)11011000}^A, \\
 &\quad I_{010111000}^A, I_{001111000}^A, I_{111011000}^A, I_{111(-1)11000}^A, \\
 &\quad \left. I_{110111000}^A, I_{101111000}^A, I_{011111000}^A, I_{111111000}^A \right)^T, \\
 I^B &= \left(I_{010011000}^B, I_{001011000}^B, I_{000111000}^B, I_{101011000}^B, \right. \\
 &\quad \left. I_{011011000}^B, I_{001111000}^B, I_{001111000}^B, I_{111011000}^B \right)
 \end{aligned}$$

$$\begin{aligned}
 & \left. I_{101111000}^B, I_{011111000}^B, I_{111111000}^B \right)^T, \\
 I^C = & \left(I_{010011000}^C, I_{(-1)10011000}^C, I_{001011000}^C, I_{101011000}^C, \right. \\
 & \left. I_{011011000}^C, I_{(-1)11011000}^C, I_{111011000}^C, I_{111(-1)11000}^C \right)^T, \\
 I^D = & \left(I_{010011000}^D, I_{001011000}^D, I_{101011000}^D, I_{011011000}^D, I_{111011000}^D \right)^T, \\
 I^E = & \left(I_{010011000}^E, I_{(-1)10011000}^E, I_{000111000}^E, I_{101011000}^E, I_{010111000}^E, \right. \\
 & \left. I_{111011000}^E, I_{111(-1)11000}^E, I_{110111000}^E, I_{101111000}^E, I_{111111000}^E \right)^T, \\
 I^F = & \left(I_{010011000}^F, I_{000111000}^F, I_{101011000}^F, I_{010111000}^F, \right. \\
 & \left. I_{111011000}^F, I_{101111000}^F, I_{111111000}^F \right)^T, \\
 I^G = & \left(I_{010011000}^G, I_{(-1)10011000}^G, I_{101011000}^G, \right. \\
 & \left. I_{111011000}^G, I_{111(-1)11000}^G \right)^T, \\
 I^H = & \left(I_{010011000}^H, I_{101011000}^H, I_{111011000}^H \right)^T. \tag{18}
 \end{aligned}$$

In the following, we will take these pre-canonical bases as our starting point. Diagrams for all master sectors are shown in Appendix A.

4.2 Master integrals of uniform transcendent weight

Below we present for all eight topologies master integrals of uniform transcendent weight. They are related to the pre-canonical basis by

$$J^X = U^X I^X, \quad X \in \{A, B, C, D, E, F, G, H\}. \tag{19}$$

The dimension of the matrix U^X is given by the number of master integrals for topology X . The matrices U^X are given in an electronic file attached to the arxiv version of this article. The master integrals of uniform transcendent weight are constructed by analysing the maximal cut in the loop-by-loop Baikov representation [37,39]. We have chosen the master integrals such that they simplify in kinematic limits (e.g. $m_N \rightarrow 0$ or $m_Z \rightarrow 0$) to the master integrals in the simpler topologies.

4.2.1 Topology A

A possible choice of master integrals of uniform transcendent weight for topology A is given by:

$$\begin{aligned}
 \text{Sector 50: } J_1^A = & \varepsilon^2 \left(\frac{m_Z^2 - t}{\mu^2} \right) \mathbf{D}^- I_{010011000}^A, \\
 J_2^A = & \varepsilon^2 \mathbf{D}^- I_{010(-1)11000}^A \\
 & - \varepsilon^2 \left(\frac{m_Z^2}{\mu^2} \right) \mathbf{D}^- I_{010011000}^A,
 \end{aligned}$$

$$\begin{aligned}
 \text{Sector 52: } J_3^A = & \varepsilon (1 + 4\varepsilon) \left(\frac{m_N^2}{\mu^2} \right) \mathbf{D}^- I_{001011000}^A, \\
 \text{Sector 56: } J_4^A = & \varepsilon^2 \left(\frac{m_Z^2}{\mu^2} \right) \mathbf{D}^- I_{000111000}^A, \\
 \text{Sector 53: } J_5^A = & -4\varepsilon^3 \left(\frac{m_N^2 - s}{\mu^2} \right) I_{101012000}^A, \\
 \text{Sector 54: } J_6^A = & \varepsilon^3 \left(\frac{r_1}{\mu^2} \right) I_{011012000}^A, \\
 J_7^A = & \varepsilon^2 \left(\frac{r_3}{\mu^2} \right) \mathbf{D}^- I_{011(-1)11000}^A \\
 & - \varepsilon^2 \left(\frac{r_3}{\mu^2} \right) \left(\frac{m_Z^2}{\mu^2} \right) \mathbf{D}^- I_{011011000}^A, \\
 \text{Sector 58: } J_8^A = & \varepsilon^2 \left(\frac{r_2}{\mu^2} \right) \left(\frac{m_Z^2}{\mu^2} \right) \mathbf{D}^- I_{010111000}^A \\
 & - \varepsilon^2 \left(\frac{r_2}{\mu^2} \right) \mathbf{D}^- I_{010011000}^A, \\
 \text{Sector 60: } J_9^A = & \varepsilon^2 \left(\frac{m_Z^2}{\mu^2} \right) \left(\frac{r_3}{\mu^2} \right) \mathbf{D}^- I_{001111000}^A \\
 & - \varepsilon^2 \left(\frac{r_3}{\mu^2} \right) \mathbf{D}^- I_{001011000}^A, \\
 \text{Sector 55: } J_{10}^A = & \varepsilon^3 \left(\frac{m_N^2 - s}{\mu^2} \right) \left(\frac{m_Z^2 - t}{\mu^2} \right) I_{111012000}^A, \\
 J_{11}^A = & \varepsilon^3 \left(\frac{m_N^2 - s}{\mu^2} \right) I_{111(-1)12000}^A \\
 & - \varepsilon^3 \left(\frac{m_N^2 - s}{\mu^2} \right) \left(\frac{m_Z^2}{\mu^2} \right) I_{111012000}^A, \\
 \text{Sector 59: } J_{12}^A = & \varepsilon^3 \left(\frac{-t}{\mu^2} \right) \left(\frac{m_Z^2}{\mu^2} \right) I_{11012000}^A, \\
 \text{Sector 61: } J_{13}^A = & \varepsilon^3 \left(\frac{m_N^2 - s}{\mu^2} \right) \left(\frac{m_Z^2}{\mu^2} \right) I_{101112000}^A, \\
 \text{Sector 62: } J_{14}^A = & \varepsilon^3 \left(\frac{r_1}{\mu^2} \right) \left(\frac{m_Z^2}{\mu^2} \right) I_{011112000}^A, \\
 \text{Sector 63: } J_{15}^A = & \varepsilon^3 \left(\frac{r_5}{\mu^4} \right) \left(\frac{m_Z^2}{\mu^2} \right) I_{111112000}^A \\
 & - \varepsilon^3 \left(\frac{r_5}{\mu^4} \right) I_{111012000}^A. \tag{20}
 \end{aligned}$$

4.2.2 Topology B

A possible choice of master integrals of uniform transcendent weight for topology B is given by:

Sector 50: $J_1^B = \varepsilon^2 \left(\frac{-t}{\mu^2}\right) I_{010022000}^B$

Sector 52: $J_2^B = \varepsilon (1 + 4\varepsilon) \left(\frac{m_N^2}{\mu^2}\right) \mathbf{D}^- I_{001011000}^B$

Sector 56: $J_3^B = \varepsilon^2 \left(\frac{m_Z^2}{\mu^2}\right) \mathbf{D}^- I_{000111000}^B$

Sector 53: $J_4^B = -4\varepsilon^3 \left(\frac{m_N^2 - s}{\mu^2}\right) I_{101012000}^B$

Sector 54: $J_5^B = \varepsilon^3 \left(\frac{r_1}{\mu^2}\right) I_{011012000}^B$

Sector 58: $J_6^B = \varepsilon^2 \left(\frac{m_Z^2}{\mu^2}\right) \left(\frac{m_Z^2 - t}{\mu^2}\right) \mathbf{D}^- I_{010111000}^B$
 $- \varepsilon^2 \left(\frac{m_Z^2}{\mu^2}\right) \mathbf{D}^- I_{010011000}^B$

Sector 60: $J_7^B = \varepsilon^2 \left(\frac{m_Z^2}{\mu^2}\right) \left(\frac{r_3}{\mu^2}\right) \mathbf{D}^- I_{001111000}^B$
 $- \varepsilon^2 \left(\frac{r_3}{\mu^2}\right) \mathbf{D}^- I_{001011000}^B$

Sector 55: $J_8^B = \varepsilon^3 \left(\frac{m_N^2 - s}{\mu^2}\right) \left(\frac{-t}{\mu^2}\right) I_{111012000}^B$

Sector 61: $J_9^B = \varepsilon^3 \left(\frac{m_N^2 - s}{\mu^2}\right) \left(\frac{m_Z^2}{\mu^2}\right) I_{101112000}^B$

Sector 62: $J_{10}^B = \varepsilon^3 \left(\frac{r_1}{\mu^2}\right) \left(\frac{m_Z^2}{\mu^2}\right) I_{011112000}^B$

Sector 63: $J_{11}^B = \varepsilon^3 \left(\frac{m_N^2 - s}{\mu^2}\right) \left(\frac{m_Z^2 - t}{\mu^2}\right) \left(\frac{m_Z^2}{\mu^2}\right) I_{111112000}^B$
 $- \varepsilon^3 \left(\frac{m_N^2 - s}{\mu^2}\right) \left(\frac{m_Z^2}{\mu^2}\right) I_{111012000}^B$ (21)

4.2.3 Topology C

A possible choice of master integrals of uniform transcendental weight for topology C is given by:

Sector 50: $J_1^C = \varepsilon^2 \left(\frac{m_Z^2 - t}{\mu^2}\right) \mathbf{D}^- I_{010011000}^C$
 $J_2^C = \varepsilon^2 \mathbf{D}^- I_{010(-1)11000}^C$

Sector 52: $J_3^C = \varepsilon (1 + 4\varepsilon) \left(\frac{m_N^2}{\mu^2}\right) \mathbf{D}^- I_{001011000}^C$

Sector 53: $J_4^C = -4\varepsilon^3 \left(\frac{m_N^2 - s}{\mu^2}\right) I_{101012000}^C$

Sector 54: $J_5^C = \varepsilon^3 \left(\frac{r_1}{\mu^2}\right) I_{011012000}^C$
 $J_6^C = \varepsilon^2 \left(\frac{r_3}{\mu^2}\right) \mathbf{D}^- I_{011(-1)11000}^C$

Sector 55: $J_7^C = \varepsilon^3 \left(\frac{m_N^2 - s}{\mu^2}\right) \left(\frac{m_Z^2 - t}{\mu^2}\right) I_{111012000}^C$
 $J_8^C = \varepsilon^3 \left(\frac{m_N^2 - s}{\mu^2}\right) I_{111(-1)12000}^C$ (22)

4.2.4 Topology D

A possible choice of master integrals of uniform transcendental weight for topology D is given by:

Sector 50: $J_1^D = \varepsilon^2 \left(\frac{-t}{\mu^2}\right) I_{010022000}^D$

Sector 52: $J_2^D = \varepsilon (1 + 4\varepsilon) \left(\frac{m_N^2}{\mu^2}\right) \mathbf{D}^- I_{001011000}^D$

Sector 53: $J_3^D = -4\varepsilon^3 \left(\frac{m_N^2 - s}{\mu^2}\right) I_{101012000}^D$

Sector 54: $J_4^D = \varepsilon^3 \left(\frac{r_1}{\mu^2}\right) I_{011012000}^D$

Sector 55: $J_5^D = \varepsilon^3 \left(\frac{m_N^2 - s}{\mu^2}\right) \left(\frac{-t}{\mu^2}\right) I_{111012000}^D$ (23)

4.2.5 Topology E

A possible choice of master integrals of uniform transcendental weight for topology E is given by:

Sector 50: $J_1^E = \varepsilon^2 \left(\frac{m_Z^2 - t}{\mu^2}\right) \mathbf{D}^- I_{010011000}^E$
 $J_2^E = \varepsilon^2 \mathbf{D}^- I_{010(-1)11000}^E$
 $- \varepsilon^2 \left(\frac{m_Z^2}{\mu^2}\right) \mathbf{D}^- I_{010011000}^E$

Sector 56: $J_3^E = \varepsilon^2 \left(\frac{m_Z^2}{\mu^2}\right) \mathbf{D}^- I_{000111000}^E$

Sector 53: $J_4^E = -4\varepsilon^3 \left(\frac{-s}{\mu^2}\right) I_{101012000}^E$

Sector 58: $J_5^E = \varepsilon^2 \left(\frac{r_2}{\mu^2}\right) \left(\frac{m_Z^2}{\mu^2}\right) \mathbf{D}^- I_{010111000}^E$
 $- \varepsilon^2 \left(\frac{r_2}{\mu^2}\right) \mathbf{D}^- I_{010011000}^E$

Sector 55: $J_6^E = \varepsilon^3 \left(\frac{-s}{\mu^2}\right) \left(\frac{m_Z^2 - t}{\mu^2}\right) I_{111012000}^E$
 $J_7^E = \varepsilon^3 \left(\frac{-s}{\mu^2}\right) I_{111(-1)12000}^E$
 $- \varepsilon^3 \left(\frac{-s}{\mu^2}\right) \left(\frac{m_Z^2}{\mu^2}\right) I_{111012000}^E$

$$\begin{aligned}
 \text{Sector 59: } J_8^E &= \varepsilon^3 \left(\frac{-t}{\mu^2}\right) \left(\frac{m_Z^2}{\mu^2}\right) I_{110112000}^E, & J_5^G &= \varepsilon^3 \left(\frac{-s}{\mu^2}\right) I_{111(-1)12000}^G. & (26) \\
 \text{Sector 61: } J_9^E &= \varepsilon^3 \left(\frac{-s}{\mu^2}\right) \left(\frac{m_Z^2}{\mu^2}\right) I_{101112000}^E, \\
 \text{Sector 63: } J_{10}^E &= \varepsilon^3 \left(\frac{r_4}{\mu^4}\right) \left(\frac{m_Z^2}{\mu^2}\right) I_{111112000}^E \\
 &\quad - \varepsilon^3 \left(\frac{r_4}{\mu^4}\right) I_{111012000}^E. & (24)
 \end{aligned}$$

4.2.6 Topology F

A possible choice of master integrals of uniform transcendental weight for topology F is given by:

$$\begin{aligned}
 \text{Sector 50: } J_1^F &= \varepsilon^2 \left(\frac{-t}{\mu^2}\right) I_{010022000}^F, \\
 \text{Sector 56: } J_2^F &= \varepsilon^2 \left(\frac{m_Z^2}{\mu^2}\right) \mathbf{D}^- I_{000111000}^F, \\
 \text{Sector 53: } J_3^F &= -4\varepsilon^3 \left(\frac{-s}{\mu^2}\right) I_{101012000}^F, \\
 \text{Sector 58: } J_4^F &= \varepsilon^2 \left(\frac{m_Z^2}{\mu^2}\right) \left(\frac{m_Z^2 - t}{\mu^2}\right) \mathbf{D}^- I_{010111000}^F \\
 &\quad - \varepsilon^2 \left(\frac{m_Z^2}{\mu^2}\right) \mathbf{D}^- I_{010011000}^F, \\
 \text{Sector 55: } J_5^F &= \varepsilon^3 \left(\frac{-s}{\mu^2}\right) \left(\frac{-t}{\mu^2}\right) I_{111012000}^F, \\
 \text{Sector 61: } J_6^F &= \varepsilon^3 \left(\frac{-s}{\mu^2}\right) \left(\frac{m_Z^2}{\mu^2}\right) I_{101112000}^F, \\
 \text{Sector 63: } J_7^F &= \varepsilon^3 \left(\frac{-s}{\mu^2}\right) \left(\frac{m_Z^2 - t}{\mu^2}\right) \left(\frac{m_Z^2}{\mu^2}\right) I_{111112000}^F \\
 &\quad - \varepsilon^3 \left(\frac{-s}{\mu^2}\right) \left(\frac{m_Z^2}{\mu^2}\right) I_{111012000}^F. & (25)
 \end{aligned}$$

4.2.7 Topology G

A possible choice of master integrals of uniform transcendental weight for topology G is given by:

$$\begin{aligned}
 \text{Sector 50: } J_1^G &= \varepsilon^2 \left(\frac{m_Z^2 - t}{\mu^2}\right) \mathbf{D}^- I_{010011000}^G, \\
 J_2^G &= \varepsilon^2 \mathbf{D}^- I_{010(-1)11000}^G, \\
 \text{Sector 53: } J_3^G &= -4\varepsilon^3 \left(\frac{-s}{\mu^2}\right) I_{101012000}^G, \\
 \text{Sector 55: } J_4^G &= \varepsilon^3 \left(\frac{-s}{\mu^2}\right) \left(\frac{m_Z^2 - t}{\mu^2}\right) I_{111012000}^G,
 \end{aligned}$$

4.2.8 Topology H

A possible choice of master integrals of uniform transcendental weight for topology H is given by:

$$\begin{aligned}
 \text{Sector 50: } J_1^H &= \varepsilon^2 \left(\frac{-t}{\mu^2}\right) I_{010022000}^H, \\
 \text{Sector 53: } J_2^H &= -4\varepsilon^3 \left(\frac{-s}{\mu^2}\right) I_{101012000}^H, \\
 \text{Sector 55: } J_3^H &= \varepsilon^3 \left(\frac{-s}{\mu^2}\right) \left(\frac{-t}{\mu^2}\right) I_{111012000}^H. & (27)
 \end{aligned}$$

5 The differential equations

The master integrals J^X satisfy a differential equation in ε -factorised form

$$dJ^X = M^X J^X, \quad X \in \{A, B, C, D, E, F, G, H\}, \quad (28)$$

with M^X of the form

$$M^X = \varepsilon \sum_{k=1}^{N_L^X} C_k^X \omega_k^X. \quad (29)$$

The differential equation is obtained as follows: Standard integration-by-parts reduction programs allow us to obtain the differential equation for the pre-canonical master integrals I^X :

$$dI^X = A^X I^X. \quad (30)$$

Integration-by-parts reduction allows us also to express any master integral J_i^X of uniform transcendental weight as defined in Sect. 4.2 as a linear combination of the pre-canonical master integrals I_j^X . This defines the matrix U^X in Eq. (19). The matrix M^X appearing in Eq. (28) is then given by

$$M^X = U^X A^X (U^X)^{-1} - U^X d (U^X)^{-1}. \quad (31)$$

The C_k^X 's appearing in Eq. (29) are square matrices with constant entries. The dimension of these matrices is given by the number of master integrals for topology X. The differential one-forms ω_k^X are of the form

$$\omega_k^X = d \log f_k^X, \quad (32)$$

where f_k^X is an algebraic function of s, t, m_Z^2, m_N^2 and μ^2 . The f_k^X 's are called letters and the set of all f_k^X 's is called the alphabet \mathcal{A}^X . The alphabets are

$$\mathcal{A}^A = \{e_1, e_2, e_4, e_6, e_7, e_9, e_{10}, e_{11}, e_{12}, e_{13}, e_{14}, e_{15}, e_{16},$$

$$\begin{aligned}
 & o_1, o_5, o_6, o_7, o_8, o_9, o_{10}, o_{11}, o_{12}, o_{13}, o_{14}, o_{15}, o_{16}, \\
 \mathcal{A}^B &= \{e_1, e_2, e_4, e_6, e_9, e_{10}, e_{11}, e_{12}, e_{13}, e_{14}, o_5, o_6, o_7, o_8, o_9\}, \\
 \mathcal{A}^C &= \{e_1, e_2, e_4, e_6, e_9, e_{10}, e_{11}, e_{12}, e_{13}, e_{14}, o_5, o_6, o_7, o_8, o_9\}, \\
 \mathcal{A}^D &= \{e_1, e_2, e_9, e_{10}, e_{11}, e_{12}, o_5, o_6\}, \\
 \mathcal{A}^E &= \{e_1, e_2, e_3, e_4, e_5, e_6, e_7, e_8, o_1, o_2, o_3, o_4\}, \\
 \mathcal{A}^F &= \{e_1, e_2, e_3, e_4, e_5, e_6\}, \\
 \mathcal{A}^G &= \{e_1, e_2, e_3, e_4, e_5, e_6\}, \\
 \mathcal{A}^H &= \{e_1, e_2, e_3\}.
 \end{aligned} \tag{33}$$

A specific letter may appear in more than one alphabet. We divide the letters in rational (or even) letters and non-rational (or odd) letters. The rational letters are

$$\begin{aligned}
 e_1 &= \frac{-s}{\mu^2}, \quad e_7 = \frac{4m_Z^2 - t}{\mu^2}, \quad e_{12} = \frac{(m_N^2 - s)^2 + st}{\mu^4}, \\
 e_2 &= \frac{-t}{\mu^2}, \quad e_8 = \frac{4m_Z^2(m_Z^2 + s) - st}{\mu^4}, \quad e_{13} = \frac{4m_N^2 - m_Z^2}{\mu^2}, \\
 e_3 &= \frac{-s - t}{\mu^2}, \quad e_9 = \frac{m_N^2}{\mu^2}, \quad e_{14} = \frac{(m_N^2 - s)^2 + sm_Z^2}{\mu^4}, \\
 e_4 &= \frac{m_Z^2}{\mu^2}, \quad e_{10} = \frac{m_N^2 - s}{\mu^2}, \quad e_{15} = \frac{m_N^2(4m_Z^2 - t) - m_Z^4}{\mu^4}, \\
 e_5 &= \frac{m_Z^2 + s}{\mu^2}, \quad e_{11} = \frac{4m_N^2 - t}{\mu^2}, \\
 e_{16} &= \frac{(4m_Z^2 - t)(m_N^2 - s)^2 + 4sm_Z^4}{\mu^6}, \\
 e_6 &= \frac{m_Z^2 - t}{\mu^2},
 \end{aligned} \tag{34}$$

The non-rational letters are

$$\begin{aligned}
 o_1 &= \frac{2m_Z^2 - t - r_2}{2m_Z^2 - t + r_2}, \\
 o_2 &= \frac{2m_Z^2(m_Z^2 + s) - st - r_4}{2m_Z^2(m_Z^2 + s) - st + r_4}, \\
 o_3 &= \frac{(4m_Z^2 - t)st + 2m_Z^4(t - s) - (2m_Z^2 - t)r_4}{(4m_Z^2 - t)st + 2m_Z^4(t - s) + (2m_Z^2 - t)r_4}, \\
 o_4 &= \frac{2m_Z^4t + st(4m_Z^2 - t) - r_2r_4}{2m_Z^4t + st(4m_Z^2 - t) + r_2r_4}, \\
 o_5 &= \frac{2m_N^2 - t - r_1}{2m_N^2 - t + r_1}, \\
 o_6 &= \frac{2m_N^2(m_N^2 - s)^2 - t(m_N^4 + s^2) - (m_N^4 - s^2)r_1}{2m_N^2(m_N^2 - s)^2 - t(m_N^4 + s^2) + (m_N^4 - s^2)r_1}, \\
 o_7 &= \frac{2m_N^2 - m_Z^2 - r_3}{2m_N^2 - m_Z^2 + r_3}, \\
 o_8 &= \frac{2m_N^2(m_Z^2 + t) - m_Z^2t - r_1r_3}{2m_N^2(m_Z^2 + t) - m_Z^2t + r_1r_3},
 \end{aligned}$$

$$\begin{aligned}
 o_9 &= \frac{2m_N^2(m_N^2 - s)^2 - m_Z^2(m_N^4 + s^2) - (m_N^4 - s^2)r_3}{2m_N^2(m_N^2 - s)^2 - m_Z^2(m_N^4 + s^2) + (m_N^4 - s^2)r_3}, \\
 o_{10} &= \frac{2m_N^2m_Z^2(4m_N^2 - m_Z^2) + [2m_N^4 - m_Z^2(4m_N^2 - m_Z^2)]t - (2m_N^2 - m_Z^2)r_1r_3}{2m_N^2m_Z^2(4m_N^2 - m_Z^2) + [2m_N^4 - m_Z^2(4m_N^2 - m_Z^2)]t + (2m_N^2 - m_Z^2)r_1r_3}, \\
 o_{11} &= \frac{-t[2m_Z^4 + (2m_N^2 - t)(4m_Z^2 - t)] - (2m_Z^2 - t)r_1r_2}{-t[2m_Z^4 + (2m_N^2 - t)(4m_Z^2 - t)] + (2m_Z^2 - t)r_1r_2}, \\
 o_{12} &= \frac{(m_N^2 - s)^2(2m_Z^2 - t) + 2sm_Z^4 - (m_N^2 - s)r_5}{(m_N^2 - s)^2(2m_Z^2 - t) + 2sm_Z^4 + (m_N^2 - s)r_5}, \\
 o_{13} &= \frac{(m_N^2 - s)^2(2m_Z^2 - 4m_Z^2t + t^2) - 2m_Z^4st - (m_N^2 - s)(2m_Z^2 - t)r_5}{(m_N^2 - s)^2(2m_Z^2 - 4m_Z^2t + t^2) - 2m_Z^4st + (m_N^2 - s)(2m_Z^2 - t)r_5}, \\
 o_{14} &= \frac{-tQ_8 - (m_N^2 + s)(2m_Z^2 - t)r_1r_5}{-tQ_8 + (m_N^2 + s)(2m_Z^2 - t)r_1r_5}, \\
 o_{15} &= \frac{-t(m_N^2 + s)m_Z^2 - r_3r_5}{-t(m_N^2 + s)m_Z^2 + r_3r_5}, \\
 o_{16} &= \frac{-t[2m_Z^4 - (m_N^2 - s)(4m_Z^2 - t)] - r_2r_5}{-t[2m_Z^4 - (m_N^2 - s)(4m_Z^2 - t)] + r_2r_5},
 \end{aligned} \tag{35}$$

with

$$\begin{aligned}
 Q_8 &= (4m_Z^2 - t) \left[2m_N^2(m_N^2 - s)^2 - t(m_N^4 + s^2) \right] \\
 &\quad + 2m_Z^4 \left((m_N^2 + s)^2 + s(4m_N^2 - t) \right).
 \end{aligned} \tag{36}$$

As an example let us write down the differential equation for topology H :

$$\begin{aligned}
 dJ^H &= M^H J^H, \\
 M^H &= \varepsilon \begin{pmatrix} 0 & 0 & 0 \\ 0 & -2 & 0 \\ 0 & -\frac{3}{4} & -1 \end{pmatrix} d \log e_1 \\
 &\quad + \varepsilon \begin{pmatrix} -2 & 0 & 0 \\ 0 & 0 & 0 \\ -\frac{3}{2} & 0 & -2 \end{pmatrix} d \log e_2 \\
 &\quad + \varepsilon \begin{pmatrix} 0 & 0 & 0 \\ 0 & 0 & 0 \\ \frac{3}{2} & \frac{3}{4} & 1 \end{pmatrix} d \log e_3.
 \end{aligned} \tag{37}$$

The differential equations for the other topologies are of a similar form. The matrices M^X for all topologies are given in an electronic file attached to the arxiv version of this article.

6 Rationalisation of the square roots

The topologies A - E contain square roots. For each topology all occurring square roots can be rationalised simultaneously. This implies that all integrals can be expressed in terms of multiple polylogarithms. For the rationalisation of the square roots we use the algorithms of [40,41].

6.1 The square root r_1

Topology D involves only the square root r_1 . The standard rationalisation of the square root r_1 is given by

$$t = -\frac{(1-y)^2}{y} m_N^2, \quad r_1 = \frac{1-y^2}{y} m_N^2, \quad (38)$$

with the inverse transformation given by

$$y = \frac{1}{2} \left(2 - \frac{t}{m_N^2} - \frac{r_1}{m_N^2} \right). \quad (39)$$

It is convenient to use instead of y the variable $\bar{y} = 1 - y$. This has the advantage that $t = 0$ corresponds to $\bar{y} = 0$. In integrating the differential equation we will choose $t = 0$ as boundary. In terms of \bar{y} we have

$$t = -\frac{\bar{y}^2}{1-\bar{y}} m_N^2, \quad r_1 = \frac{\bar{y}(2-\bar{y})}{1-\bar{y}} m_N^2. \quad (40)$$

The inverse transformation is given by

$$\bar{y} = \frac{t+r_1}{2m_N^2}. \quad (41)$$

6.2 The square roots r_1 and r_3

Topologies B and C involve the square roots r_1 and r_3 . The square root r_1 is rationalised as above, the square root r_3 is rationalised by

$$m_Z^2 = \frac{(1+z)^2}{z} m_N^2, \quad r_3 = \frac{1-z^2}{z} m_N^2. \quad (42)$$

The inverse transformation is given by

$$z = -\frac{1}{2} \left(2 - \frac{m_Z^2}{m_N^2} + \frac{r_3}{m_N^2} \right). \quad (43)$$

6.3 The square roots r_2 and r_4

Topology E involves the square roots r_2 and r_4 . The square root r_2 is rationalised by

$$t = -\frac{\tilde{y}^2}{1-\tilde{y}} m_Z^2, \quad r_2 = \frac{\tilde{y}(2-\tilde{y})}{1-\tilde{y}} m_Z^2. \quad (44)$$

The inverse transformation is given by

$$\tilde{y} = \frac{t+r_2}{2m_Z^2}. \quad (45)$$

The square root r_4 is rationalised by

$$m_Z^2 = \frac{(1-2\tilde{z})(2-\tilde{y})^2}{4\tilde{z}^2(1-\tilde{y})} s, \quad r_4 = \frac{(1-\tilde{z})(1-2\tilde{z})\tilde{y}(2-\tilde{y})^3}{4\tilde{z}^3(1-\tilde{y})^2} s^2. \quad (46)$$

The inverse transformation is given by

$$\tilde{z} = -\frac{(4m_Z^2-t)}{4m_Z^2} \left(\frac{s}{m_Z^2} - \frac{r_4}{m_Z^2 r_2} \right). \quad (47)$$

6.4 The square roots r_1, r_2, r_3 and r_5

Topology A involves the square roots r_1, r_2, r_3 and r_5 . The square roots r_1 and r_2 are rationalised by

$$t = -\frac{(\hat{y}^2 m_Z^2 - m_N^2)^2}{\hat{y}(1+\hat{y})(m_N^2 + \hat{y} m_Z^2)}, \quad r_1 = \frac{(\hat{y}^2 m_Z^2 - m_N^2)((1+2\hat{y})m_N^2 + \hat{y}^2 m_Z^2)}{\hat{y}(1+\hat{y})(m_N^2 + \hat{y} m_Z^2)}, \quad r_2 = \frac{(\hat{y}^2 m_Z^2 - m_N^2)(m_N^2 + \hat{y}(2+\hat{y})m_Z^2)}{\hat{y}(1+\hat{y})(m_N^2 + \hat{y} m_Z^2)}. \quad (48)$$

The inverse transformation is given by

$$\hat{y} = -\frac{t^2 - t(r_1+r_2) + r_1 r_2}{4m_Z^2 t}. \quad (49)$$

The root r_3 is rationalised as in Sect. 6.2:

$$m_Z^2 = \frac{(1+z)^2}{z} m_N^2, \quad r_3 = \frac{1-z^2}{z} m_N^2. \quad (50)$$

The inverse transformation is given by

$$z = -\frac{1}{2} \left(2 - \frac{m_Z^2}{m_N^2} + \frac{r_3}{m_N^2} \right). \quad (51)$$

Finally, the root r_5 is rationalised by

$$s = \frac{\hat{x}}{(1+\hat{x})} \left(m_N^2 + \hat{x} \frac{m_Z^4}{4m_Z^2 - t} \right), \quad r_5 = \frac{-t}{(1+\hat{x})r_2} \left[m_N^2 (4m_Z^2 - t) + \hat{x} (2+\hat{x}) m_Z^4 \right]. \quad (52)$$

The occurrence of r_2 on the right-hand side is unproblematic, as r_2 is rationalised by Eq. (48). The inverse transformation is given by

$$\hat{x} = -\frac{1}{2m_Z^4} \left[(m_N^2 - s)(4m_Z^2 - t) + \frac{r_2 r_5}{t} \right]. \quad (53)$$

7 Boundary values

In order to solve the differential equation, we need boundary values. As boundary point we choose

$$t = 0, \quad m_N^2 = 0, \quad m_Z^2 = \infty. \quad (54)$$

There are four master integrals with a trivial kinematic dependence. These integrals are easily calculated with the help of the Feynman parametrisation. We find

$$\begin{aligned}
 J_1^H &= e^{2\varepsilon\gamma_E} \left(\frac{-t}{\mu^2}\right)^{-2\varepsilon} \frac{\Gamma(1+2\varepsilon)\Gamma(1-\varepsilon)^3}{\Gamma(1-3\varepsilon)}, \\
 J_2^H &= e^{2\varepsilon\gamma_E} \left(\frac{-s}{\mu^2}\right)^{-2\varepsilon} \frac{\Gamma(1+2\varepsilon)\Gamma(1+\varepsilon)\Gamma(1-2\varepsilon)\Gamma(1-\varepsilon)^2}{\Gamma(1-3\varepsilon)}, \\
 J_2^F &= e^{2\varepsilon\gamma_E} \left(\frac{m_Z^2}{\mu^2}\right)^{-2\varepsilon} \Gamma(1+2\varepsilon)\Gamma(1+\varepsilon)\Gamma(1-\varepsilon), \\
 J_2^D &= \frac{3}{2}e^{2\varepsilon\gamma_E} \left(\frac{m_N^2}{\mu^2}\right)^{-2\varepsilon} \frac{\Gamma(1+2\varepsilon)\Gamma(1+\varepsilon)\Gamma(1-\varepsilon)^2\Gamma(1-4\varepsilon)}{\Gamma(1-2\varepsilon)\Gamma(1-3\varepsilon)}. \tag{55}
 \end{aligned}$$

The boundary values of the master integrals of intermediate complexity we compute with the help of the Mellin–Barnes representation. We illustrate this for the example of the master integral J_6^F . For this integral we obtain the Mellin–Barnes representation

$$\begin{aligned}
 J_6^F &= -e^{2\varepsilon\gamma_E} \varepsilon^2 \frac{\Gamma(1+\varepsilon)\Gamma(1-\varepsilon)^2}{\Gamma(1-2\varepsilon)} \left(\frac{m_Z^2}{\mu^2}\right)^{-2\varepsilon} \\
 &\quad \times \frac{1}{2\pi i} \int d\sigma \left(\frac{-s}{m_Z^2}\right)^{\sigma+1} \\
 &\quad \times \frac{\Gamma(-\sigma)\Gamma(-\sigma-1-2\varepsilon)\Gamma(\sigma+1)^2\Gamma(\sigma+2+2\varepsilon)}{\Gamma(\sigma+2-\varepsilon)}. \tag{56}
 \end{aligned}$$

The integration contour runs from $-i\infty$ to $+i\infty$ and separates the poles of $\Gamma(-\sigma)$ and $\Gamma(-\sigma-1-2\varepsilon)$ from the poles of $\Gamma(\sigma+1)$ and $\Gamma(\sigma+2+2\varepsilon)$. For $|s| < m_Z^2$ we may close the integration contour to the right and sum up the residues of $\Gamma(-\sigma)$ and $\Gamma(-\sigma-1-2\varepsilon)$. For the boundary value we are only interested in the leading term in an expansion in $1/m_Z^2$. The leading term is given by the first residue of $\Gamma(-\sigma-1-2\varepsilon)$ located at

$$\sigma = -1 - 2\varepsilon. \tag{57}$$

We therefore obtain

$$\begin{aligned}
 J_6^F &= -\frac{1}{4}e^{2\varepsilon\gamma_E} \frac{\Gamma(1+2\varepsilon)\Gamma(1+\varepsilon)\Gamma(1-\varepsilon)^2\Gamma(1-2\varepsilon)}{\Gamma(1-3\varepsilon)} \\
 &\quad \times \left(\frac{-s}{\mu^2}\right)^{-2\varepsilon} + O\left(\frac{-s}{m_Z^2}\right). \tag{58}
 \end{aligned}$$

The boundary values of the more complicated integrals we obtain from regularity conditions. For example, the boundary values for J_3^H are determined from the condition that this integral is regular at $e_3 = 0$, this corresponds to the condition that there is no singularity whenever the Mandelstam variable

u vanishes. This follows from physics: As the master integral is a planar integral, there is no singularity in the crossed u -channel.

8 Results

We set $\mu^2 = s$. The values of the Feynman integrals at another scale μ_1^2 are easily obtained through

$$J(\mu_1^2) = e^{2\varepsilon L} J(\mu^2) \text{ with } L = \ln\left(\frac{\mu_1^2}{\mu^2}\right). \tag{59}$$

8.1 Integrating the differential equation

As already mentioned in Sect. 7, we use

$$t = 0, \quad m_N^2 = 0, \quad m_Z^2 = \infty \tag{60}$$

as boundary point. After setting $\mu^2 = s$ the Feynman integrals depend only on dimensionless kinematic variables, which we may take as

$$x_t = \frac{-t}{s}, \quad x_{m_N^2} = \frac{m_N^2}{s}, \quad x_{m_Z^2}^{-1} = \frac{s}{m_Z^2}. \tag{61}$$

Our chosen boundary point corresponds to

$$(x_t, x_{m_N^2}, x_{m_Z^2}^{-1}) = (0, 0, 0). \tag{62}$$

The rationalisation of square roots will introduce a change of variables. By a suitable definition of the new variables we may ensure that the boundary point in the new variables is still $(0, 0, 0)$. Let us now assume that our integration variables are (x_1, x_2, x_3) . We then fix an integration path γ : We first integrate along x_1 at $x_2 = x_3 = 0$, followed by an integration along x_2 at $x_1 = \text{const}$ and $x_3 = 0$ and finally an integration along x_3 at $x_1 = \text{const}$ and $x_2 = \text{const}$.

8.1.1 Integration for topologies B-H

In Table 3 we show for topologies B - H the dimensionless kinematic variables and the integration order.

For topologies B and C we use the variable \bar{y} from Sect. 6.1 and the variable z from Sect. 6.2. The variable \bar{y} from Sect. 6.1 is also used for topology D . For topology E we use the variables \bar{y} and \bar{z} from Sect. 6.3. The rationalisation of the square roots turns the arguments of the dlog-forms given in Eq. (32) into rational functions. This implies that all iterated integrals from the integration of the differential equation can be expressed in terms of multiple polylogarithms. Multiple polylogarithms are defined as follows: One first defines

Table 3 The dimensionless kinematic variables and the integration order for topologies *B-H*

Topologies	Variables and integration order
<i>B, C</i>	$(x_{m_N^2}, z, \bar{y})$
<i>D</i>	$(x_{m_N^2}, \bar{y})$
<i>E</i>	(\tilde{z}, \tilde{y})
<i>F, G</i>	$(x_{m_Z^2}^{-1}, x_t)$
<i>H</i>	(x_t)

$G(0, \dots, 0; y)$ with k zeros to be

$$G(0, \dots, 0; y) = \frac{1}{k!} (\ln y)^k. \tag{63}$$

This includes the trivial case $G(; y) = 1$. Multiple polylogarithms are then defined recursively by

$$G(z_1, z_2, \dots, z_k; y) = \int_0^y \frac{dy_1}{y_1 - z_1} G(z_2, \dots, z_k; y_1). \tag{64}$$

A multiple polylogarithm $G(z_1, \dots, z_k; y)$ is said to have a trailing zero if $z_k = 0$. Using the shuffle product, we may isolate trailing zeros in powers of

$$G(0; y) = \ln y. \tag{65}$$

An example is given by

$$G(z, 0; y) = \ln y \cdot G(z; y) - G(0, z; y). \tag{66}$$

For multiple polylogarithms without a trailing zero we have the scaling identity

$$G(z_1, \dots, z_k; y) = G\left(\frac{z_1}{y}, \dots, \frac{z_k}{y}; 1\right) \tag{67}$$

A multiple polylogarithm $G(z_1, \dots, z_k; 1)$ has a convergent power series expansion if $z_1 \neq 1$ and

$$|z_j| \geq 1 \text{ for all } j \in \{1, \dots, k\}. \tag{68}$$

The kinematic variables and the integration order for topologies *B-H* have been chosen such that after isolating all trailing zeros in powers of logarithms, the remaining multiple polylogarithms have convergent power series expansions in the kinematic region of interest. This ensures a highly efficient numerical evaluation. Furthermore, since we have for small values of $(-t)$

$$-t \sim \bar{y}^2 \sim \tilde{y}^2 \tag{69}$$

and since we have for large values of m_Z^2

$$m_Z^2 \sim z^{-1} \sim \tilde{z}^{-2} \tag{70}$$

this procedure also makes the large logarithms

$$\ln\left(\frac{-t}{s}\right) \text{ and } \ln\left(\frac{s}{m_Z^2}\right) \tag{71}$$

manifest. As an example one finds

$$\begin{aligned} J_7^F = & -\frac{5}{4} + \left(2L_t - \frac{1}{2}i\pi\right)\varepsilon + \left(-L_t^2 + 2i\pi L_t + \frac{15}{4}\zeta_2\right)\varepsilon^2 \\ & + \left(-2i\pi L_t^2 - 12\zeta_2 L_t + \frac{89}{6}\zeta_3 - \frac{1}{12}i\pi^3\right)\varepsilon^3 \\ & + \left[\frac{1}{3}L_t^4 + \frac{4}{3}i\pi L_t^3 + 11\zeta_2 L_t^2 - \left(\frac{70}{3}\zeta_3 + \frac{1}{3}i\pi^3\right)L_t\right. \\ & \left. + \frac{493}{16}\zeta_4 + \frac{19}{3}i\pi\zeta_3\right]\varepsilon^4 \\ & + O\left(x_{m_Z^2}^{-1}\right) + O(x_t) + O(\varepsilon^5), \end{aligned} \tag{72}$$

with $L_t = \ln(-t/s)$.

8.1.2 Integration for topology A

For topologies *B-H* we were in the lucky situation that with our choice of variables all multiple polylogarithms had convergent power series expansions in the kinematic region of interest. This is no longer straightforward for topology *A*.

The variables \hat{x}, \hat{y}, z from Sect. 6.4 rationalise all square roots for topology *A*. This allows us to conclude that all integrals from topology *A* can be expressed in terms of multiple polylogarithms and that all master integrals from topology *A* are of uniform weight. The latter statement uses the fact that the boundary constants are of uniform weight as well [42]. As the master integrals $J_{11}^A - J_{13}^A$ appear also in other topologies, the new information is the statement that the master integrals J_{14}^A and J_{15}^A can be expressed in term of multiple polylogarithms and are of uniform weight.

The polynomials appearing in the dlog-forms after rationalisation suggest the integration order

$$(z, \hat{y}, \hat{x}). \tag{73}$$

This integration order has the property that for each integration we encounter at most quadratic polynomials in the integration variable. However, the resulting expression in terms of multiple polylogarithms involves multiple polylogarithms which do not have convergent power series expansions in the kinematic region of interest. This is not a fundamental problem, as we may transform these multiple polylogarithms such that they do have a convergent power series expansion. However, these transformations are rather slow.

Choosing other integration orders will result in polynomials of higher degree in the integration variables. While we may determine the roots of these polynomials numerically, there is a second drawback: Factorising these polynomials into linear factors will significantly increase the number of

terms. To give an example: Consider an iterated integral of depth w , where each dlog-form has as argument a polynomial of degree N in the integration variable. A single iterated integral of this type will lead to N^w terms. This growth prevents an efficient numerical evaluation.

An efficient numerical evaluation routine for the kinematic region of interest is achieved as follows: We introduce the variable

$$v = \sqrt{x_t} \tag{74}$$

and integrate the differential equation with the integration order

$$(x_{m_N^2}, z, v). \tag{75}$$

The first two integrations are done at $t = 0$ and give multiple polylogarithms. From the definition of the square roots in Eq. (13) we see that at $t = 0$ only the square root r_3 is non-zero. The square root r_3 is rationalised by the change of variables from m_Z^2 to z given in Eq. (42). There is one subtlety: The ($t \rightarrow 0$)-limit of the letters o_{11} , o_{14} and o_{16} is not a rational function of $x_{m_N^2}$ and z . However, in the differential equation these letters always multiply the integrals J_6^A , J_8^A and J_{14}^A . These integrals vanish at $t = 0$ and as a consequence the letters o_{11} , o_{14} and o_{16} do not appear in the result for the master integrals at $t = 0$.

For the last integration in v we have the integration kernels

$$\{e_2, e_6, e_7, e_{11}, e_{12}, e_{15}, e_{16}, o_1, o_5, o_6, o_8, o_{10}, o_{11}, o_{12}, o_{13}, o_{14}, o_{15}, o_{16}\}. \tag{76}$$

$d \ln(e_2)$ has a simple pole at $v = 0$, all others have Taylor expansions in v . The Taylor expansions are convergent for

$$|t| < \min \left\{ 4m_N^2, m_Z^2, \left| \frac{m_Z^2 (4m_N^2 - m_Z^2)}{m_N^2} \right|, \left| \frac{(m_N^2 - s)^2}{s} \right|, \times \left| \frac{4m_Z^2 [(m_N^2 - s)^2 + sm_Z^2]}{(m_N^2 - s)^2} \right| \right\}. \tag{77}$$

This includes the kinematic region of the P2 experiment. For large m_Z^2 , the most stringent condition is

$$|t| < \left| \frac{(m_N^2 - s)^2}{s} \right|. \tag{78}$$

This is nothing else than the condition on the physical region [43].

8.2 Numerical results

For the numerical evaluation we have written for each topology a C++-program, which uses the GiNaC-library [44]. This allows numerical evaluations with arbitrary precision.

The algorithms for the numerical evaluation of multiple polylogarithms are based on [45], topology A uses in addition the class `user_defined_kernel` from Ref. [46] for the last integration over the variable v .

As a typical kinematical point we use

$$s = 1.18 \text{ GeV}^2, \quad t = -4.5 \cdot 10^{-3} \text{ GeV}^2, \\ m_Z^2 = 8.32 \cdot 10^3 \text{ GeV}^2, \quad m_N^2 = 0.867 \text{ GeV}^2. \tag{79}$$

This corresponds to the kinematics of the P2 experiment with an electron beam of $E_{\text{beam}} = 155 \text{ MeV}$ and momentum transfer of $Q^2 = -t = 4.5 \cdot 10^{-3} \text{ GeV}^2$. The Mandelstam variable s is then given by

$$s = (E_{\text{beam}} + m_N)^2. \tag{80}$$

We use

$$m_N = 0.931 \text{ GeV}, \quad m_Z = 91.2 \text{ GeV}. \tag{81}$$

The values of the master integrals for the first five terms of the ϵ -expansion at the kinematic point specified by Eq. (79) are given to 8 digits in Tables 4, 5, 6, 7, 8, 9, 10, and 11. In addition, we compared our results to the results of the program `AMFlow` [47–49] to 50 digits and found perfect agreement. Our numerical evaluation routines are significantly faster than `AMFlow`. For example, our program takes about eight seconds to evaluate all master integrals of topology A to 50 digits up to and including the ϵ^4 -term. The corresponding evaluation with `AMFlow` takes about 21 minutes. All calculations were done on a single core of a standard desktop computer.

8.3 Large logarithms

In the kinematic region of interest (i.e. small $(-t)$ and large m_Z^2)

$$\ln\left(\frac{-t}{s}\right) \text{ and } \ln\left(\frac{s}{m_Z^2}\right) \tag{82}$$

are large logarithms. Below we list for all master integrals the leading logarithms. At order ϵ^j we can have at most j powers of large logarithms. The leading logarithms are the ones which occur to power j at order ϵ^j . We remark that this counting defines at order ϵ^0 constants as leading logarithms. In some topologies we use different variables. Since we have for small values of $(-t)$

$$-t \sim \bar{y}^2 \sim \tilde{y}^2 \tag{83}$$

and since we have for large values of m_Z^2

$$m_Z^2 \sim z^{-1} \sim \tilde{z}^{-2} \tag{84}$$

the discussion carries over in a straightforward way to the new variables. Let us stress that the following formulae are

Table 4 Numerical results for the first five terms of the ε -expansion of the master integrals $J_1^A - J_{15}^A$ for the kinematic point specified by Eq. (79)

	ε^0	ε^1	ε^2	ε^3	ε^4
J_1^A	1	-17.721808	161.96604	-1018.2849	4958.5733
J_2^A	-1	17.721806	-161.96601	1018.2846	-4958.5714
J_3^A	1.5	0.92469222	12.622024	20.886482	133.48343
J_4^A	1	-17.721806	161.96601	-1018.2846	4958.5715
J_5^A	0.5	2.3459023 +6.2831853i	-20.695763 +33.35282i	-152.3306 +57.516544i	-545.47467 -73.412472i
J_6^A	0	0	-0.00015280111	0.00094650525	-0.0070979484
J_7^A	0	-18.337851	153.5486	-1032.1747	4869.4159
J_8^A	0	0.002941742	-0.052132982	0.47646222	-2.9955308
J_9^A	0	18.337851	-153.54859	1032.1747	-4869.4155
J_{10}^A	-0.125	-0.58647531 -1.5707963i	5.17355 -8.3382329i	38.08511 -14.379368i	136.35187 +18.352165i
J_{11}^A	0	0	0.00039275926 +3.1349531e - 05i	-0.0024636613 +0.00026046032i	0.016696228 +0.0010683564i
J_{12}^A	0	2.7043262e - 07	-3.9812567e - 06	3.0234529e - 05	-0.00015754108
J_{13}^A	-0.125	-0.58647558 -1.5707963i	5.1735479 -8.3382363i	38.085115 -14.379397i	136.35197 +18.35205i
J_{14}^A	0	0	-0.00013778848	0.00069534307	-0.0049161254
J_{15}^A	0	0	0.00016537254 +1.4597012e - 05i	-0.00085429938 +0.00012127593i	0.0052303379 +0.00049744992i

Table 5 Numerical results for the first five terms of the ε -expansion of the master integrals $J_1^B - J_{11}^B$ for the kinematic point specified by Eq. (79)

	ε^0	ε^1	ε^2	ε^3	ε^4
J_1^B	1	11.138385	60.386872	199.16752	381.04712
J_2^B	1.5	0.92469222	12.622024	20.886482	133.48343
J_3^B	1	-17.721806	161.96601	-1018.2846	4958.5715
J_4^B	0.5	2.3459023 +6.2831853i	-20.695763 +33.35282i	-152.3306 +57.516544i	-545.47467 -73.412472i
J_5^B	0	0	-9.3465893	-122.24172	-894.31476
J_6^B	1	39.998578	-41.192268	1416.62	-4196.4777
J_7^B	0	18.337851	-153.54859	1032.1747	-4869.4155
J_8^B	-1.125	-10.113215 -4.712389i	-34.840045 -52.488401i	-15.424624 -282.51753i	354.88999 -923.44496i
J_9^B	-0.125	-0.58647558 -1.5707963i	5.1735479 -8.3382363i	38.085115 -14.379397i	136.35197 +18.35205i
J_{10}^B	0	0	-9.3464365	-122.24267	-894.30774
J_{11}^B	-0.625	-6.1556684 -1.5707963i	-28.400251 -26.654035i	-48.368222 -173.96566i	100.24132 -633.98226i

Table 6 Numerical results for the first five terms of the ε -expansion of the master integrals $J_1^C - J_8^C$ for the kinematic point specified by Eq. (79)

	ε^0	ε^1	ε^2	ε^3	ε^4
J_1^C	1	-17.721808	161.96604	-1018.2849	4958.5733
J_2^C	-1	17.721806	-161.96601	1018.2846	-4958.5714
J_3^C	1.5	0.92469222	12.622024	20.886482	133.48343
J_4^C	0.5	2.3459023 +6.2831853i	-20.695763 +33.35282i	-152.3306 +57.516544i	-545.47467 -73.412472i
J_5^C	0	0	-0.00015280111	0.00094650525	-0.0070979484
J_6^C	0	-18.337851	153.5486	-1032.1747	4869.4159
J_7^C	-0.125	-0.58647531 -1.5707963i	5.17355 -8.3382329i	38.08511 -14.379368i	136.35187 +18.352165i
J_8^C	0	0	0.00039275926 +3.1349531e - 05i	-0.0024636613 +0.00026046032i	0.016696228 +0.0010683564i

Table 7 Numerical results for the first five terms of the ε -expansion of the master integrals $J_1^D - J_5^D$ for the kinematic point specified by Eq. (79)

	ε^0	ε^1	ε^2	ε^3	ε^4
J_1^D	1	11.138385	60.386872	199.16752	381.04712
J_2^D	1.5	0.92469222	12.622024	20.886482	133.48343
J_3^D	0.5	2.3459023 +6.2831853i	-20.695763 +33.35282i	-152.3306 +57.516544i	-545.47467 -73.412472i
J_4^D	0	0	-9.3465893	-122.24172	-894.31476
J_5^D	-1.125	-10.113215 -4.712389i	-34.840045 -52.488401i	-15.424624 -282.51753i	354.88999 -923.44496i

Table 8 Numerical results for the first five terms of the ε -expansion of the master integrals $J_1^E - J_{10}^E$ for the kinematic point specified by Eq. (79)

	ε^0	ε^1	ε^2	ε^3	ε^4
J_1^E	1	-17.721808	161.96604	-1018.2849	4958.5733
J_2^E	-1	17.721806	-161.96601	1018.2846	-4958.5714
J_3^E	1	-17.721806	161.96601	-1018.2846	4958.5715
J_4^E	1	6.2831853i	-18.094275	-10.417826 -31.006277i	21.375884 -65.457134i
J_5^E	0	0.002941742	-0.052132982	0.47646222	-2.9955308
J_6^E	-0.25	5.4086524e - 07 -1.5707963i	4.5221719 -0.00044213247i	2.6153956 +7.7502428i	-5.4032243 +16.362486i
J_7^E	0	0	0.0013984474 +0.00044553083i	-0.01094393 +0.0013366082i	0.059232976 +0.0018112415i
J_8^E	0	2.7043262e - 07	-3.9812567e - 06	3.0234529e - 05	-0.00015754108
J_9^E	-0.25	-1.5707963i	4.5221702 -0.00044553083i	2.6154006 +7.7502326i	-5.4032039 +16.362472i
J_{10}^E	0	0	0.00015520336 +5.5026642e - 05i	-0.0010587544 +0.00016508381i	0.004771572 +0.00022371167i

Table 9 Numerical results for the first five terms of the ε -expansion of the master integrals $J_1^F - J_7^F$ for the kinematic point specified by Eq. (79)

	ε^0	ε^1	ε^2	ε^3	ε^4
J_1^F	1	11.138385	60.386872	199.16752	381.04712
J_2^F	1	-17.721806	161.96601	-1018.2846	4958.5715
J_3^F	1	6.2831853i	-18.094275	-10.417826	21.375884
				-31.006277i	-65.457134i
J_4^F	1	39.998578	-41.192268	1416.62	-4196.4777
J_5^F	-2.25	-16.707577	-30.485748	195.29664	1596.8385
		-4.712389i	-52.488401i	-284.3299i	-937.45111i
J_6^F	-0.25	-1.5707963i	4.5221702	2.6154006	-5.4032039
			-0.00044553083i	+7.7502326i	+16.362472i
J_7^F	-1.25	-11.138386	-24.846011	127.58233	1069.9622
		-1.5707963i	-34.991825i	-197.30353i	-641.33006i

Table 10 Numerical results for the first five terms of the ε -expansion of the master integrals $J_1^G - J_5^G$ for the kinematic point specified by Eq. (79)

	ε^0	ε^1	ε^2	ε^3	ε^4
J_1^G	1	-17.721808	161.96604	-1018.2849	4958.5733
J_2^G	-1	17.721806	-161.96601	1018.2846	-4958.5714
J_3^G	1	6.2831853i	-18.094275	-10.417826	21.375884
				-31.006277i	-65.457134i
J_4^G	-0.25	5.4086524e - 07	4.5221719	2.6153956	-5.4032243
		-1.5707963i	-0.00044213247i	+7.7502428i	+16.362486i
J_5^G	0	0	0.0013984474	-0.01094393	0.059232976
			+0.00044553083i	+0.0013366082i	+0.0018112415i

Table 11 Numerical results for the first five terms of the ε -expansion of the master integrals $J_1^H - J_3^H$ for the kinematic point specified by Eq. (79)

	ε^0	ε^1	ε^2	ε^3	ε^4
J_1^H	1	11.138385	60.386872	199.16752	381.04712
J_2^H	1	6.2831853i	-18.094275	-10.417826	21.375884
				-31.006277i	-65.457134i
J_3^H	-2.25	-16.707577	-30.485748	195.29664	1596.8385
		-4.712389i	-52.488401i	-284.3299i	-937.45111i

provided only to quickly gauge the numerical importance of all master integrals. The analytic results are exact and can be used to extract not only the leading logarithms, but also all sub-leading ones as well as the non-logarithmic part. We use the following notation:

$$L_t = \ln\left(\frac{-t}{s}\right), \quad L_Z = \ln\left(\frac{s}{m_Z^2}\right),$$

$$L_{\bar{y}} = \ln(\bar{y}), \quad L_z = \ln(z), \quad L_{\bar{z}} = \ln(\bar{z}). \quad (85)$$

Comparing the expressions for the leading logarithms with the numerical results from Sect. 8.2 we see – as expected – a correlation between large logarithms and large numerical values.

8.3.1 Topology A

$$J_1^A = 1 + 2L_z\varepsilon + 2L_z^2\varepsilon^2 + \frac{4}{3}L_z^3\varepsilon^3 + \frac{2}{3}L_z^4\varepsilon^4 + \text{subleading} + O(\varepsilon^5),$$

$$J_2^A = -1 - 2L_z\varepsilon - 2L_z^2\varepsilon^2 - \frac{4}{3}L_z^3\varepsilon^3 - \frac{2}{3}L_z^4\varepsilon^4 + \text{subleading} + O(\varepsilon^5),$$

$$J_3^A = \frac{3}{2} + \text{subleading} + O(\varepsilon^5),$$

$$J_4^A = 1 + 2L_z\varepsilon + 2L_z^2\varepsilon^2 + \frac{4}{3}L_z^3\varepsilon^3 + \frac{2}{3}L_z^4\varepsilon^4$$

$$\begin{aligned}
 & +\text{subleading} + O(\varepsilon^5), \\
 J_5^A &= \frac{1}{2} + \text{subleading} + O(\varepsilon^5), \\
 J_6^A &= 0 + \text{subleading} + O(\varepsilon^5), \\
 J_7^A &= 2L_z\varepsilon + 2L_z^2\varepsilon^2 + \frac{4}{3}L_z^3\varepsilon^3 \\
 & \quad + \frac{2}{3}L_z^4\varepsilon^4 + \text{subleading} + O(\varepsilon^5), \\
 J_8^A &= 0 + \text{subleading} + O(\varepsilon^5), \\
 J_9^A &= -2L_z\varepsilon - 2L_z^2\varepsilon^2 - \frac{4}{3}L_z^3\varepsilon^3 \\
 & \quad - \frac{2}{3}L_z^4\varepsilon^4 + \text{subleading} + O(\varepsilon^5), \\
 J_{10}^A &= -\frac{1}{8} + \text{subleading} + O(\varepsilon^5), \\
 J_{11}^A &= 0 + \text{subleading} + O(\varepsilon^5), \\
 J_{12}^A &= 0 + \text{subleading} + O(\varepsilon^5), \\
 J_{13}^A &= -\frac{1}{8} + \text{subleading} + O(\varepsilon^5), \\
 J_{14}^A &= 0 + \text{subleading} + O(\varepsilon^5), \\
 J_{15}^A &= 0 + \text{subleading} + O(\varepsilon^5). \tag{86}
 \end{aligned}$$

8.3.2 Topology B

$$\begin{aligned}
 J_1^B &= 1 - 4L_{\bar{y}}\varepsilon + 8L_{\bar{y}}^2\varepsilon^2 - \frac{32}{3}L_{\bar{y}}^3\varepsilon^3 \\
 & \quad + \frac{32}{3}L_{\bar{y}}^4\varepsilon^4 + \text{subleading} + O(\varepsilon^5), \\
 J_2^B &= \frac{3}{2} + \text{subleading} + O(\varepsilon^5), \\
 J_3^B &= 1 + 2L_z\varepsilon + 2L_z^2\varepsilon^2 + \frac{4}{3}L_z^3\varepsilon^3 \\
 & \quad + \frac{2}{3}L_z^4\varepsilon^4 + \text{subleading} + O(\varepsilon^5), \\
 J_4^B &= \frac{1}{2} + \text{subleading} + O(\varepsilon^5), \\
 J_5^B &= 0 + \text{subleading} + O(\varepsilon^5), \\
 J_6^B &= 1 - (2L_z + 8L_{\bar{y}})\varepsilon - (2L_z^2 - 16L_{\bar{y}}^2)\varepsilon^2 \\
 & \quad - \left(\frac{4}{3}L_z^3 + \frac{64}{3}L_{\bar{y}}^3\right)\varepsilon^3 - \left(\frac{2}{3}L_z^4 - \frac{64}{3}L_{\bar{y}}^4\right)\varepsilon^4 \\
 & \quad + \text{subleading} + O(\varepsilon^5), \\
 J_7^B &= -2L_z\varepsilon - 2L_z^2\varepsilon^2 - \frac{4}{3}L_z^3\varepsilon^3 \\
 & \quad - \frac{2}{3}L_z^4\varepsilon^4 + \text{subleading} + O(\varepsilon^5),
 \end{aligned}$$

$$\begin{aligned}
 J_8^B &= -\frac{9}{8} + 3L_{\bar{y}}\varepsilon - 3L_{\bar{y}}^2\varepsilon^2 \\
 & \quad + 4L_{\bar{y}}^4\varepsilon^4 + \text{subleading} + O(\varepsilon^5), \\
 J_9^B &= -\frac{1}{8} + \text{subleading} + O(\varepsilon^5), \\
 J_{10}^B &= 0 + \text{subleading} + O(\varepsilon^5), \\
 J_{11}^B &= -\frac{5}{8} + 2L_{\bar{y}}\varepsilon - 2L_{\bar{y}}^2\varepsilon^2 \\
 & \quad + \frac{8}{3}L_{\bar{y}}^4\varepsilon^4 + \text{subleading} + O(\varepsilon^5). \tag{87}
 \end{aligned}$$

8.3.3 Topology C

$$\begin{aligned}
 J_1^C &= 1 + 2L_z\varepsilon + 2L_z^2\varepsilon^2 + \frac{4}{3}L_z^3\varepsilon^3 \\
 & \quad + \frac{2}{3}L_z^4\varepsilon^4 + \text{subleading} + O(\varepsilon^5), \\
 J_2^C &= -1 - 2L_z\varepsilon - 2L_z^2\varepsilon^2 - \frac{4}{3}L_z^3\varepsilon^3 \\
 & \quad - \frac{2}{3}L_z^4\varepsilon^4 + \text{subleading} + O(\varepsilon^5), \\
 J_3^C &= \frac{3}{2} + \text{subleading} + O(\varepsilon^5), \\
 J_4^C &= \frac{1}{2} + \text{subleading} + O(\varepsilon^5), \\
 J_5^C &= 0 + \text{subleading} + O(\varepsilon^5), \\
 J_6^C &= 2L_z\varepsilon + 2L_z^2\varepsilon^3 + \frac{4}{3}L_z^3\varepsilon^3 \\
 & \quad + \frac{2}{3}L_z^4\varepsilon^4 + \text{subleading} + O(\varepsilon^5), \\
 J_7^C &= -\frac{1}{8} + \text{subleading} + O(\varepsilon^5), \\
 J_8^C &= 0 + \text{subleading} + O(\varepsilon^5). \tag{88}
 \end{aligned}$$

8.3.4 Topology D

$$\begin{aligned}
 J_1^D &= 1 - 4L_{\bar{y}}\varepsilon + 8L_{\bar{y}}^2\varepsilon^2 - \frac{32}{3}L_{\bar{y}}^3\varepsilon^3 \\
 & \quad + \frac{32}{3}L_{\bar{y}}^4\varepsilon^4 + \text{subleading} + O(\varepsilon^5), \\
 J_2^D &= \frac{3}{2} + \text{subleading} + O(\varepsilon^5), \\
 J_3^D &= \frac{1}{2} + \text{subleading} + O(\varepsilon^5), \\
 J_4^D &= 0 + \text{subleading} + O(\varepsilon^5), \\
 J_5^D &= -\frac{9}{8} + 3L_{\bar{y}}\varepsilon - 3L_{\bar{y}}^2\varepsilon^2 \\
 & \quad + 4L_{\bar{y}}^4\varepsilon^4 + \text{subleading} + O(\varepsilon^5). \tag{89}
 \end{aligned}$$

8.3.5 Topology E

$$\begin{aligned}
 J_1^E &= 1 + 4L_{\bar{z}}\varepsilon + 8L_{\bar{z}}^2\varepsilon^2 + \frac{32}{3}L_{\bar{z}}^3\varepsilon^3 \\
 &\quad + \frac{32}{3}L_{\bar{z}}^4\varepsilon^4 + \text{subleading} + O(\varepsilon^5), \\
 J_2^E &= -1 - 4L_{\bar{z}}\varepsilon - 8L_{\bar{z}}^2\varepsilon^2 - \frac{32}{3}L_{\bar{z}}^3\varepsilon^3 \\
 &\quad - \frac{32}{3}L_{\bar{z}}^4\varepsilon^4 + \text{subleading} + O(\varepsilon^5), \\
 J_3^E &= 1 + 4L_{\bar{z}}\varepsilon + 8L_{\bar{z}}^2\varepsilon^2 + \frac{32}{3}L_{\bar{z}}^3\varepsilon^3 \\
 &\quad + \frac{32}{3}L_{\bar{z}}^4\varepsilon^4 + \text{subleading} + O(\varepsilon^5), \\
 J_4^E &= 1 + \text{subleading} + O(\varepsilon^5), \\
 J_5^E &= 0 + \text{subleading} + O(\varepsilon^5), \\
 J_6^E &= -\frac{1}{4} + \text{subleading} + O(\varepsilon^5), \\
 J_7^E &= 0 + \text{subleading} + O(\varepsilon^5), \\
 J_8^E &= 0 + \text{subleading} + O(\varepsilon^5), \\
 J_9^E &= -\frac{1}{4} + \text{subleading} + O(\varepsilon^5), \\
 J_{10}^E &= 0 + \text{subleading} + O(\varepsilon^5).
 \end{aligned} \tag{90}$$

8.3.6 Topology F

$$\begin{aligned}
 J_1^F &= 1 - 2L_t\varepsilon + 2L_t^2\varepsilon^2 - \frac{4}{3}L_t^3\varepsilon^3 \\
 &\quad + \frac{2}{3}L_t^4\varepsilon^4 + \text{subleading} + O(\varepsilon^5), \\
 J_2^F &= 1 + 2L_Z\varepsilon + 2L_Z^2\varepsilon^2 + \frac{4}{3}L_Z^3\varepsilon^3 \\
 &\quad + \frac{2}{3}L_Z^4\varepsilon^4 + \text{subleading} + O(\varepsilon^5), \\
 J_3^F &= 1 + \text{subleading} + O(\varepsilon^5), \\
 J_4^F &= 1 - (2L_Z + 4L_t)\varepsilon - (2L_Z^2 - 4L_t^2)\varepsilon^2 \\
 &\quad - \left(\frac{4}{3}L_Z^3 + \frac{8}{3}L_t^3\right)\varepsilon^3 - \left(\frac{2}{3}L_Z^4 - \frac{4}{3}L_t^4\right)\varepsilon^4 \\
 &\quad + \text{subleading} + O(\varepsilon^5), \\
 J_5^F &= -\frac{9}{4} + 3L_t\varepsilon - \frac{3}{2}L_t^2\varepsilon^2 \\
 &\quad + \frac{1}{2}L_t^4\varepsilon^4 + \text{subleading} + O(\varepsilon^5), \\
 J_6^F &= -\frac{1}{4} + \text{subleading} + O(\varepsilon^5), \\
 J_7^F &= -\frac{5}{4} + 2L_t\varepsilon - L_t^2\varepsilon^2
 \end{aligned}$$

$$+ \frac{1}{3}L_t^4\varepsilon^4 + \text{subleading} + O(\varepsilon^5). \tag{91}$$

8.3.7 Topology G

$$\begin{aligned}
 J_1^G &= 1 + 2L_Z\varepsilon + 2L_Z^2\varepsilon^2 + \frac{4}{3}L_Z^3\varepsilon^3 \\
 &\quad + \frac{2}{3}L_Z^4\varepsilon^4 + \text{subleading} + O(\varepsilon^5), \\
 J_2^G &= -1 - 2L_Z\varepsilon - 2L_Z^2\varepsilon^2 - \frac{4}{3}L_Z^3\varepsilon^3 \\
 &\quad - \frac{2}{3}L_Z^4\varepsilon^4 + \text{subleading} + O(\varepsilon^5), \\
 J_3^G &= 1 + \text{subleading} + O(\varepsilon^5), \\
 J_4^G &= -\frac{1}{4} + \text{subleading} + O(\varepsilon^5), \\
 J_5^G &= 0 + \text{subleading} + O(\varepsilon^5).
 \end{aligned} \tag{92}$$

8.3.8 Topology H

$$\begin{aligned}
 J_1^H &= 1 - 2L_t\varepsilon + 2L_t^2\varepsilon^2 - \frac{4}{3}L_t^3\varepsilon^3 \\
 &\quad + \frac{2}{3}L_t^4\varepsilon^4 + \text{subleading} + O(\varepsilon^5), \\
 J_2^H &= 1 + \text{subleading} + O(\varepsilon^5), \\
 J_3^H &= -\frac{9}{4} + 3L_t\varepsilon - \frac{3}{2}L_t^2\varepsilon^2 \\
 &\quad + \frac{1}{2}L_t^4\varepsilon^4 + \text{subleading} + O(\varepsilon^5).
 \end{aligned} \tag{93}$$

9 Conclusions

In this paper we computed a set of two-loop Feynman integrals relevant to the Moller experiment and to the P2 experiment. We considered Feynman integrals, which are obtained from a box integral by the insertion of a light fermion loop. The exchanged particles in the box integral are either photons or heavy electro-weak gauge bosons. We considered all combinations. By rationalising all occurring square roots we showed that all these Feynman integrals can be expressed in terms of multiple polylogarithms. We organised our results such that all large logarithms are manifest. Furthermore, we provided highly efficient numerical evaluation routines for all master integrals in the kinematic region of interest.

For the complete set of the two-loop electro-weak corrections there are of course more diagrams to be considered. In particular, this includes the planar and non-planar double box integrals. Again, one has to consider all possible combinations of photon and heavy gauge boson exchanges. The case of the exchange of three heavy gauge bosons is particularly interesting: We expect the planar double box integral

with the exchange of three heavy gauge bosons to be associated with a curve of genus one and the non-planar double box integral with the exchange of three heavy gauge bosons to be associated with a curve of genus two [50]. This is an interesting project for the future.

Acknowledgements We would like to thank Jens Erler, Mikhail Gorchtein and Hubert Spiesberger for useful discussions and comments on the manuscript. This work has been supported by the Cluster of Excellence Precision Physics, Fundamental Interactions, and Structure of Matter (PRISMA EXC 2118/1) funded by the German Research Foundation (DFG) within the German Excellence Strategy (Project ID 390831469).

Data Availability Statement This manuscript has associated data in a data repository. [Authors' comment: This manuscript has associated data in a repository, see appendix B].

Code Availability Statement This manuscript has associated data in a data repository. [Authors' comment: This manuscript has associated code in a repository, see appendix B].

Open Access This article is licensed under a Creative Commons Attribution 4.0 International License, which permits use, sharing, adaptation, distribution and reproduction in any medium or format, as long as you give appropriate credit to the original author(s) and the source, provide a link to the Creative Commons licence, and indicate if changes were made. The images or other third party material in this article are included in the article's Creative Commons licence, unless indicated otherwise in a credit line to the material. If material is not included in the article's Creative Commons licence and your intended use is not permitted by statutory regulation or exceeds the permitted use, you will need to obtain permission directly from the copyright holder. To view a copy of this licence, visit <http://creativecommons.org/licenses/by/4.0/>.
Funded by SCOAP³.

Appendix A: Master sectors

In this appendix we show in Figs. 4, 5 and 6 the diagrams of all master sectors. The colour coding is as follows: A green line indicates a particle of mass m_N , a red line a particle of mass m_Z . Uncoloured lines are massless.

Appendix B: Supplementary material

Attached to the arxiv version of this article are for each topology

$$X \in \{A, B, C, D, E, F, G, H\} \tag{94}$$

the electronic files

`topo_X_symbolic.mpl`, `topo_X_numeric.cc`.

The first file is in Maple syntax and defines the transformation matrix U^X appearing in eq. (19), its inverse $(U^X)^{-1}$ and the matrix M^X appearing in the differential equation (28). These are denoted as

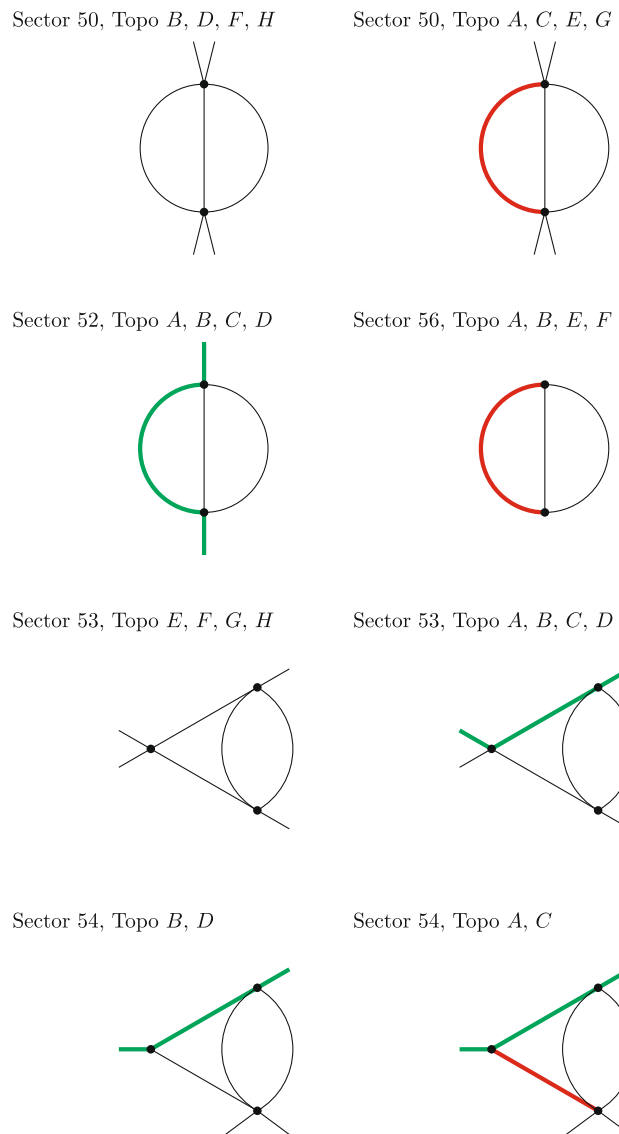


Fig. 4 Master sectors (part 1)

`U_X`, `Uinv_X`, `M_X`.

The second file `topo_X_numeric.cc` is a C++-program and provides numerical evaluation routines for all master integrals of a given topology. This C++-program requires the GiNaC-library [44].

Appendix C: One-loop integrals

For convenience we also include the corresponding one-loop integrals. At one-loop we consider the family of integrals

$$I_{\nu_1 \nu_2 \nu_3 \nu_4} = e^{\gamma_E \epsilon} (\mu^2)^{\nu - \frac{D}{2}} \int \frac{d^D k_1}{i\pi^{\frac{D}{2}}} \prod_{j=1}^4 \frac{1}{P_j^{\nu_j}}, \tag{95}$$

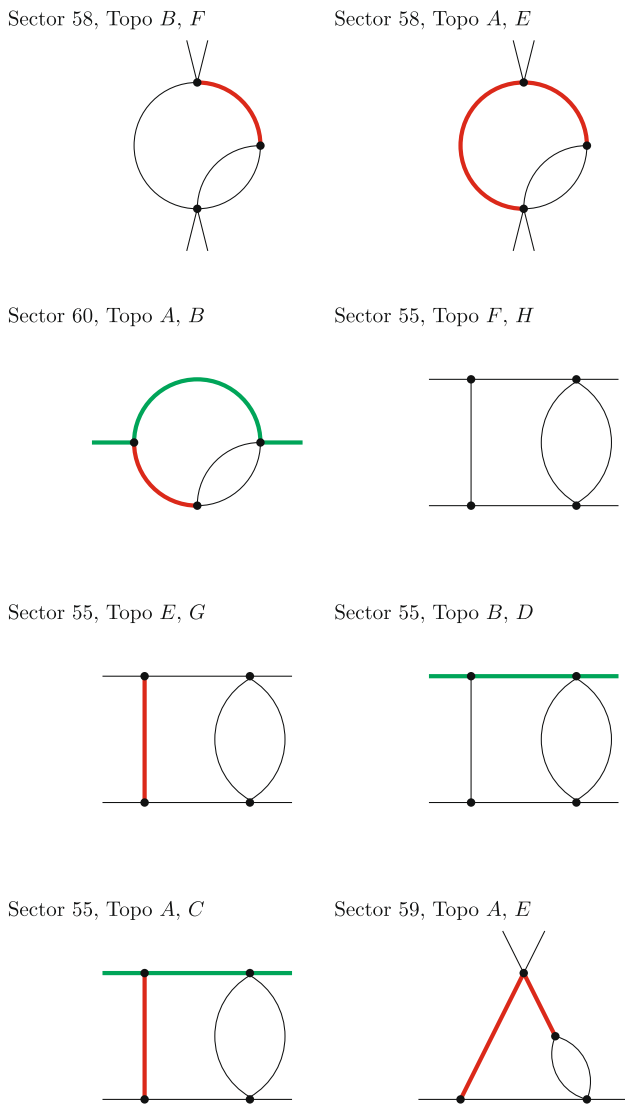


Fig. 5 Master sectors (part 2)

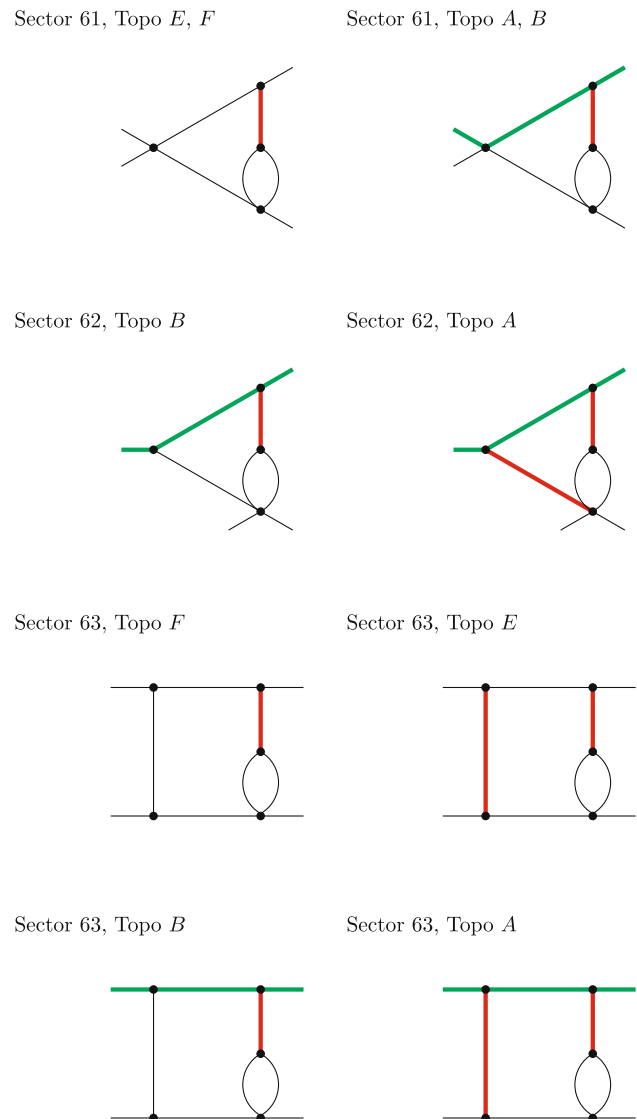


Fig. 6 Master sectors (part 3)

where the notation is as in Sect. 2. At one-loop, the topologies B and C are related by symmetry, and so are the topologies F and G . We therefore have to consider only the topologies A, B, D, E, F and H . Possible pre-canonical bases are:

$$\begin{aligned}
 K^A &= \left(I_{0100}^A, I_{0010}^A, I_{1010}^A, I_{0110}^A, I_{0101}^A, I_{1110}^A, I_{1101}^A, I_{0111}^A, I_{1111}^A \right)^T, \\
 K^B &= \left(I_{0010}^B, I_{0001}^B, I_{1010}^B, I_{0101}^B, I_{0011}^B, I_{1011}^B, I_{0111}^B, I_{1111}^B \right)^T, \\
 K^D &= \left(I_{0010}^D, I_{1010}^D, I_{0101}^D, I_{0111}^D, I_{1111}^D \right)^T, \\
 K^E &= \left(I_{0100}^E, I_{1010}^E, I_{0101}^E, I_{1110}^E, I_{1101}^E, I_{1111}^E \right)^T, \\
 K^F &= \left(I_{0001}^F, I_{1010}^F, I_{0101}^F, I_{1011}^F, I_{1111}^F \right)^T, \\
 K^H &= \left(I_{1010}^H, I_{0101}^H, I_{1111}^H \right)^T.
 \end{aligned} \tag{96}$$

Below we list a possible choice of master integrals of uniform transcendent weight, together with the corresponding leading logarithms. For the logarithms we use the same notation as in Sect. 8.3.

C.1 Topology A

$$\begin{aligned}
 \text{Sector 2: } L_1^A &= \varepsilon \mathbf{D}^- I_{0100}^A \\
 &= 1 + L_z \varepsilon + \frac{1}{2} L_z^2 \varepsilon^2 \\
 &\quad + \text{subleading} + O(\varepsilon^3), \\
 \text{Sector 4: } L_2^A &= \varepsilon \mathbf{D}^- I_{0010}^A \\
 &= 1 + \text{subleading} + O(\varepsilon^3),
 \end{aligned}$$

$$\begin{aligned}
 \text{Sector 5: } L_3^A &= \varepsilon \left(\frac{m_N^2 - s}{\mu^2} \right) \mathbf{D}^- I_{1010}^A \\
 &= -1 + \text{subleading} + O(\varepsilon^3), \\
 \text{Sector 6: } L_4^A &= \varepsilon \left(\frac{r_3}{\mu^2} \right) \mathbf{D}^- I_{0110}^A \\
 &= -L_z \varepsilon - \frac{1}{2} L_z^2 \varepsilon^2 \\
 &\quad + \text{subleading} + O(\varepsilon^3), \\
 \text{Sector 10: } L_5^A &= \varepsilon \left(\frac{r_2}{\mu^2} \right) \mathbf{D}^- I_{0101}^A \\
 &= 0 + \text{subleading} + O(\varepsilon^3), \\
 \text{Sector 7: } L_6^A &= \varepsilon^2 \left(\frac{m_N^2 - s}{\mu^2} \right) I_{1110}^A \\
 &= 0 + \text{subleading} + O(\varepsilon^3), \\
 \text{Sector 11: } L_7^A &= \varepsilon^2 \left(\frac{-t}{\mu^2} \right) I_{1101}^A \\
 &= 0 + \text{subleading} + O(\varepsilon^3), \\
 \text{Sector 14: } L_8^A &= \varepsilon^2 \left(\frac{r_1}{\mu^2} \right) I_{0111}^A \\
 &= 0 + \text{subleading} + O(\varepsilon^3), \\
 \text{Sector 15: } L_9^A &= \varepsilon^2 \left(\frac{r_5}{\mu^4} \right) I_{1111}^A \\
 &= 0 + \text{subleading} + O(\varepsilon^3). \tag{97}
 \end{aligned}$$

C.2 Topology B

$$\begin{aligned}
 \text{Sector 4: } L_1^B &= \varepsilon \mathbf{D}^- I_{0010}^B \\
 &= 1 + \text{subleading} + O(\varepsilon^3), \\
 \text{Sector 8: } L_2^B &= \varepsilon \mathbf{D}^- I_{0001}^B \\
 &= 1 + L_z \varepsilon + \frac{1}{2} L_z^2 \varepsilon^2 \\
 &\quad + \text{subleading} + O(\varepsilon^3), \\
 \text{Sector 5: } L_3^B &= \varepsilon \left(\frac{m_N^2 - s}{\mu^2} \right) \mathbf{D}^- I_{1010}^B \\
 &= -1 + \text{subleading} + O(\varepsilon^3), \\
 \text{Sector 10: } L_4^B &= \varepsilon \left(\frac{m_Z^2 - t}{\mu^2} \right) \mathbf{D}^- I_{0101}^B \\
 &= -1 - L_z \varepsilon - \frac{1}{2} L_z^2 \varepsilon^2 \\
 &\quad + \text{subleading} + O(\varepsilon^3),
 \end{aligned}$$

$$\begin{aligned}
 \text{Sector 12: } L_5^B &= \varepsilon \left(\frac{r_3}{\mu^2} \right) \mathbf{D}^- I_{0011}^B \\
 &= -L_z \varepsilon - \frac{1}{2} L_z^2 \varepsilon^2 \\
 &\quad + \text{subleading} + O(\varepsilon^3), \\
 \text{Sector 13: } L_6^B &= \varepsilon^2 \left(\frac{m_N^2 - s}{\mu^2} \right) I_{1011}^B \\
 &= 0 + \text{subleading} + O(\varepsilon^3), \\
 \text{Sector 14: } L_7^B &= \varepsilon^2 \left(\frac{r_1}{\mu^2} \right) I_{0111}^B \\
 &= 0 + \text{subleading} + O(\varepsilon^3), \\
 \text{Sector 15: } L_8^B &= \varepsilon^2 \left(\frac{m_N^2 - s}{\mu^2} \right) \left(\frac{m_Z^2 - t}{\mu^2} \right) I_{1111}^B \\
 &= \frac{1}{2} + \text{subleading} + O(\varepsilon^3). \tag{98}
 \end{aligned}$$

C.3 Topology D

$$\begin{aligned}
 \text{Sector 4: } L_1^D &= \varepsilon \mathbf{D}^- I_{0010}^D \\
 &= 1 + \text{subleading} + O(\varepsilon^3), \\
 \text{Sector 5: } L_2^D &= \varepsilon \left(\frac{m_N^2 - s}{\mu^2} \right) \mathbf{D}^- I_{1010}^D \\
 &= -1 + \text{subleading} + O(\varepsilon^3), \\
 \text{Sector 10: } L_3^D &= \varepsilon \left(\frac{-t}{\mu^2} \right) \mathbf{D}^- I_{0101}^D \\
 &= -2 + 4L_{\bar{y}} \varepsilon - 4L_{\bar{y}}^2 \varepsilon^2 \\
 &\quad + \text{subleading} + O(\varepsilon^3), \\
 \text{Sector 14: } L_4^D &= \varepsilon^2 \left(\frac{r_1}{\mu^2} \right) I_{0111}^D \\
 &= 0 + \text{subleading} + O(\varepsilon^3), \\
 \text{Sector 15: } L_5^D &= \varepsilon^2 \left(\frac{m_N^2 - s}{\mu^2} \right) \left(\frac{-t}{\mu^2} \right) I_{1111}^D \\
 &= 2 - 2L_{\bar{y}} \varepsilon + \text{subleading} + O(\varepsilon^3). \tag{99}
 \end{aligned}$$

C.4 Topology E

$$\begin{aligned}
 \text{Sector 2: } L_1^E &= \varepsilon \mathbf{D}^- I_{0100}^E \\
 &= 1 + 2L_{\bar{z}} \varepsilon + 2L_{\bar{z}}^2 \varepsilon^2 \\
 &\quad + \text{subleading} + O(\varepsilon^3), \\
 \text{Sector 5: } L_2^E &= \varepsilon \left(\frac{-s}{\mu^2} \right) \mathbf{D}^- I_{1010}^E
 \end{aligned}$$

$$\begin{aligned}
 &= -2 + \text{subleading} + O(\varepsilon^3), \\
 \text{Sector 10: } L_3^E &= \varepsilon \left(\frac{r_2}{\mu^2} \right) \mathbf{D}^- I_{0101}^E \\
 &= 0 + \text{subleading} + O(\varepsilon^3), \\
 \text{Sector 7: } L_4^E &= \varepsilon^2 \left(\frac{-s}{\mu^2} \right) I_{1110}^E \\
 &= 0 + \text{subleading} + O(\varepsilon^3), \\
 \text{Sector 11: } L_5^E &= \varepsilon^2 \left(\frac{-t}{\mu^2} \right) I_{1101}^E \\
 &= 0 + \text{subleading} + O(\varepsilon^3), \\
 \text{Sector 15: } L_6^E &= \varepsilon^2 \left(\frac{r_4}{\mu^4} \right) I_{1111}^E \\
 &= 0 + \text{subleading} + O(\varepsilon^3). \tag{100}
 \end{aligned}$$

C.5 Topology F

$$\begin{aligned}
 \text{Sector 8: } L_1^F &= \varepsilon \mathbf{D}^- I_{0001}^F \\
 &= 1 + L_Z \varepsilon + \frac{1}{2} L_Z^2 \varepsilon^2 \\
 &\quad + \text{subleading} + O(\varepsilon^3), \\
 \text{Sector 5: } L_2^F &= \varepsilon \left(\frac{-s}{\mu^2} \right) \mathbf{D}^- I_{1010}^F \\
 &= -2 + \text{subleading} + O(\varepsilon^3), \\
 \text{Sector 10: } L_3^F &= \varepsilon \left(\frac{m_Z^2 - t}{\mu^2} \right) \mathbf{D}^- I_{0101}^F \\
 &= -1 - L_Z \varepsilon - \frac{1}{2} L_Z^2 \varepsilon^2 \\
 &\quad + \text{subleading} + O(\varepsilon^3), \\
 \text{Sector 13: } L_4^F &= \varepsilon^2 \left(\frac{-s}{\mu^2} \right) I_{1011}^F \\
 &= 0 + \text{subleading} + O(\varepsilon^3), \\
 \text{Sector 15: } L_5^F &= \varepsilon^2 \left(\frac{-s}{\mu^2} \right) \left(\frac{m_Z^2 - t}{\mu^2} \right) I_{1111}^F \\
 &= 1 + \text{subleading} + O(\varepsilon^3). \tag{101}
 \end{aligned}$$

C.6 Topology H

$$\begin{aligned}
 \text{Sector 5: } L_1^H &= \varepsilon \left(\frac{-s}{\mu^2} \right) \mathbf{D}^- I_{1010}^H \\
 &= -2 + \text{subleading} + O(\varepsilon^3), \\
 \text{Sector 10: } L_2^H &= \varepsilon \left(\frac{-t}{\mu^2} \right) \mathbf{D}^- I_{0101}^H
 \end{aligned}$$

$$\begin{aligned}
 &= -2 + 2L_t \varepsilon - L_t^2 \varepsilon^2 \\
 &\quad + \text{subleading} + O(\varepsilon^3), \\
 \text{Sector 15: } L_3^H &= \varepsilon^2 \left(\frac{-s}{\mu^2} \right) \left(\frac{-t}{\mu^2} \right) I_{1111}^H \\
 &= 4 - 2L_t \varepsilon + \text{subleading} + O(\varepsilon^3). \tag{102}
 \end{aligned}$$

References

1. MOLLER, J. Benesch et al., (2014). [arXiv:1411.4088](#)
2. D. Becker et al., Eur. Phys. J. A **54**, 208 (2018). [arXiv:1802.04759](#)
3. I. Dubovyk, A. Freitas, J. Gluza, T. Riemann, J. Usovitsch, Phys. Lett. B **762**, 184 (2016). [arXiv:1607.08375](#)
4. Y. Du, A. Freitas, H.H. Patel, M.J. Ramsey-Musolf, Phys. Rev. Lett. **126**, 131801 (2021). [arXiv:1912.08220](#)
5. J. Erler, R. Ferro-Hernández, A. Freitas, JHEP **08**, 183 (2022). [arXiv:2202.11976](#)
6. I. Dubovyk et al., Phys. Rev. D **106**, L111301 (2022). [arXiv:2201.02576](#)
7. T. Armadillo, R. Bonciani, S. Devoto, N. Rana, A. Vicini, Comput. Phys. Commun. **282**, 108545 (2023). [arXiv:2205.03345](#)
8. A.G. Aleksejevs, S.G. Barkanova, Y.M. Bystritskiy, E.A. Kuraev, V.A. Zykunov, Phys. Part. Nucl. Lett. **12**, 645 (2015). [arXiv:1504.03560](#)
9. A.G. Aleksejevs et al., Eur. Phys. J. C **72**, 2249 (2012)
10. A.V. Kotikov, Phys. Lett. B **254**, 158 (1991)
11. A.V. Kotikov, Phys. Lett. B **267**, 123 (1991). [Erratum: Phys. Lett. B **295**, 409 (1992)]
12. T. Gehrmann, E. Remiddi, Nucl. Phys. B **580**, 485 (2000). [arXiv:hep-ph/9912329](#)
13. K.G. Chetyrkin, F.V. Tkachov, Nucl. Phys. B **192**, 159 (1981)
14. J.M. Henn, Phys. Rev. Lett. **110**, 251601 (2013). [arXiv:1304.1806](#)
15. A. Smirnov, JHEP **10**, 107 (2008). [arXiv:0807.3243](#)
16. A.V. Smirnov, F.S. Chuharev, Comput. Phys. Commun. **247**, 106877 (2020). [arXiv:1901.07808](#)
17. R.N. Lee, (2012). [arXiv:1212.2685](#)
18. R.N. Lee, J. Phys. Conf. Ser. **523**, 012059 (2014). [arXiv:1310.1145](#)
19. C. Studerus, Comput. Phys. Commun. **181**, 1293 (2010). [arXiv:0912.2546](#)
20. A. von Manteuffel, C. Studerus, (2012). [arXiv:1201.4330](#)
21. P. Maierhöfer, J. Usovitsch, P. Uwer, Comput. Phys. Commun. **230**, 99 (2018). [arXiv:1705.05610](#)
22. J. Klappert, F. Lange, P. Maierhöfer, J. Usovitsch, Comput. Phys. Commun. **266**, 108024 (2021). [arXiv:2008.06494](#)
23. T. Peraro, JHEP **12**, 030 (2016). [arXiv:1608.01902](#)
24. T. Peraro, JHEP **07**, 031 (2019). [arXiv:1905.08019](#)
25. W.J. Marciano, A. Sirlin, Phys. Rev. D **27**, 552 (1983)
26. W.J. Marciano, A. Sirlin, Phys. Rev. D **29**, 75 (1984). [Erratum: Phys. Rev. D **31**, 213 (1985)]
27. J. Erler, A. Kurylov, M.J. Ramsey-Musolf, Phys. Rev. D **68**, 016006 (2003). [arXiv:hep-ph/0302149](#)
28. H.Q. Zhou, C.W. Kao, S.N. Yang, K. Nagata, Phys. Rev. C **81**, 035208 (2010). [arXiv:0910.3307](#)
29. B.C. Rislow, C.E. Carlson, Phys. Rev. D **83**, 113007 (2011). [arXiv:1011.2397](#)
30. P.G. Blunden, W. Melnitchouk, A.W. Thomas, Phys. Rev. Lett. **107**, 081801 (2011). [arXiv:1102.5334](#)
31. N.L. Hall, P.G. Blunden, W. Melnitchouk, A.W. Thomas, R.D. Young, Phys. Lett. B **753**, 221 (2016). [arXiv:1504.03973](#)

32. M. Gorchtein, H. Spiesberger, Phys. Rev. C **94**, 055502 (2016). [arXiv:1608.07484](#)
33. J. Erler, M. Gorchtein, O. Koshchii, C.-Y. Seng, H. Spiesberger, Phys. Rev. D **100**, 053007 (2019). [arXiv:1907.07928](#)
34. O.V. Tarasov, Phys. Rev. D **54**, 6479 (1996). [arXiv:hep-th/9606018](#)
35. O.V. Tarasov, Nucl. Phys. B **502**, 455 (1997). [arXiv:hep-ph/9703319](#)
36. C. Bogner, S. Weinzierl, Int. J. Mod. Phys. A **25**, 2585 (2010). [arXiv:1002.3458](#)
37. S. Weinzierl, *Feynman Integrals* (Springer, 2022). [arXiv:2201.03593](#)
38. S. Laporta, Int. J. Mod. Phys. A **15**, 5087 (2000). [arXiv:hep-ph/0102033](#)
39. H. Frellesvig, C.G. Papadopoulos, JHEP **04**, 083 (2017). [arXiv:1701.07356](#)
40. M. Besier, D. Van Straten, S. Weinzierl, Commun. Number Theor. Phys. **13**, 253 (2019). [arXiv:1809.10983](#)
41. M. Besier, P. Wasser, S. Weinzierl, Comput. Phys. Commun. **253**, 107197 (2020). [arXiv:1910.13251](#)
42. H. Frellesvig, S. Weinzierl, (2023). [arXiv:2301.02264](#)
43. E. Byckling, K. Kajantie, *Particle Kinematics* (Wiley, 1973)
44. C. Bauer, A. Frink, R. Kreckel, J. Symb. Comput. **33**, 1 (2002). [arXiv:cs.sc/0004015](#)
45. J. Vollinga, S. Weinzierl, Comput. Phys. Commun. **167**, 177 (2005). [arXiv:hep-ph/0410259](#)
46. M. Walden, S. Weinzierl, Comput. Phys. Commun. **265**, 108020 (2021). [arXiv:2010.05271](#)
47. X. Liu, Y.-Q. Ma, Comput. Phys. Commun. **283**, 108565 (2023). [arXiv:2201.11669](#)
48. X. Liu, Y.-Q. Ma, C.-Y. Wang, Phys. Lett. B **779**, 353 (2018). [arXiv:1711.09572](#)
49. Z.-F. Liu, Y.-Q. Ma, Phys. Rev. Lett. **129**, 222001 (2022). [arXiv:2201.11637](#)
50. R. Marzucca, A.J. McLeod, B. Page, S. Pögel, S. Weinzierl, (2023). [arXiv:2307.11497](#)